

# FEATURE EXTRACTION FROM ECG SIGNAL USING WAVELET TRANSFORMS

**A DISSERTATION**

*Submitted in partial fulfillment of the  
requirements for the award of the degree*

*of*

**MASTER OF ENGINEERING**

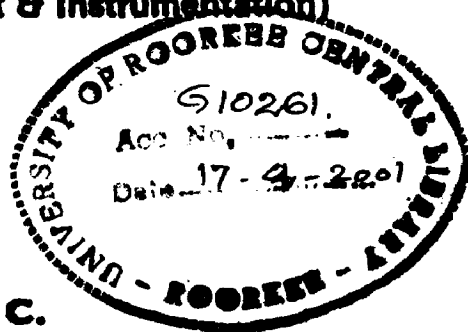
*in*

**ELECTRICAL ENGINEERING**

**(With Specialization in Measurement & Instrumentation)**

**By**

**JAYA KRISHNA C.**



**DEPARTMENT OF ELECTRICAL ENGINEERING  
UNIVERSITY OF ROORKEE  
ROORKEE-247 667 (INDIA)**

**FEBRUARY, 2001**

**CANDIDATE'S DECLARATION**

I hereby declare that the work which is being presented in the project entitled "FEATURE EXTRACTION FROM ECG SIGNAL USING WAVELET TRANSFORMS" in partial fulfilment of the requirements for the award of the degree of **MASTER OF ENGINEERING** with specialization in **MEASUREMENT AND INSTRUMENTATION** submitted in the Department of Electrical Engineering, University of Roorkee, Roorkee, is an authentic record of my own work carried out from July-2000 to January-2001 under the guidance of **Dr. S. C. Saxena**, Professor and **Dr. Vinod Kumar**, Professor, Department of Electrical Engineering, University of Roorkee, Roorkee.


The matter embodied in this project has not been submitted by me for the award of any other degree.

Date : 26/2/2001

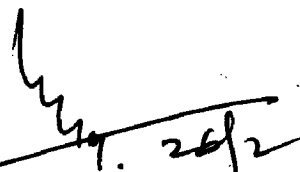
Place : Roorkee

C. Jaya Krishna  
(JAYA KRISHNA C.)

This is to certify that the above statement made by the candidate is correct to the best of our knowledge.

  
(Dr. S. C. SAXENA)  
26/2/2001

Professor  
Department of Electrical Engg.  
University of Roorkee  
Roorkee - 247 667

  
(Dr. VINOD KUMAR)  
26/2

Professor  
Department of Electrical Engg  
University of Roorkee  
Roorkee - 247 667

## ACKNOWLEDGEMENT

---

I express deep sense of gratitude towards my supervisors **Dr. S. C. Saxena**, Professor and **Dr. Vinod Kumar**, Professor, Department of Electrical Engineering, University of Roorkee, Roorkee, for their invaluable guidance, support and continued thought providing discussions at every juncture in carrying out this work.

My sincere thanks are due to all Faculty members of Measurement & Instrumentation Group of Department of Electrical Engineering, for their invaluable suggestions from time to time.

Special thanks to Mr. S. T. Hamde, Ph.D. Scholar, for providing the necessary literature during the course of this work.

I am also grateful to Mr.V.K. Giri, Ph.D. Scholar , for giving me full support in completing this work.

I am highly indebted to my mother and family members for providing moral support and encouragement during the course of this work.

Date : 26/2/2001

Place : Roorkee

*C. Jaya Krishna*  
(JAYA KRISHNA C.)

# CONTENTS

---

	Page No.
<b>CANDIDATE'S DECLARATION</b>	<b>i</b>
<b>ACKNOWLEDGEMENT</b>	<b>ii</b>
<b>CONTENTS</b>	<b>iii</b>
<b>ABSTRACT</b>	<b>vi</b>
<b>Chapter 1 INTRODUCTION</b>	<b>1</b>
1.1 Electrocardiogram	1
1.2 Discrete wavelet transforms	3
1.3 Organization of Dissertation	4
<b>Chapter 2 ELECTROCARDIOGRAM</b>	<b>6</b>
2.1 Introduction	6
2.2 Heart Physiology and Functions	6
2.3 The Electrocardiogram	7
2.4 Recording of ECG	8
2.4.1 Bipolar Standard Limb Leads	9
2.4.2 Unipolar Leads	9
2.4.3 Unipolar Chest Leads	10
2.4.4 Orthogonal Leads	10
2.5 Noise Artifacts in ECG	15
2.6 The CSE Database	15
2.7 Conclusions	16
<b>Chapter 3 WAVELET TRANSFORMS</b>	<b>17</b>
3.1 Introduction	17

3.2	Fourier Transforms	17
3.3	Short Time Fourier Transform	19
3.4	Continuous Wavelet Transforms	22
3.5	Discrete Wavelet Transforms	25
3.6	conclusions	31
<b>Chapter 4</b>	<b>PRE-PROCESSING OF ECG SIGNAL</b>	<b>32</b>
4.1	Introduction	32
4.2	Sources of Noise	32
4.2.1	Power line Interference	32
4.2.2	Muscle Artifacts	33
4.2.3	Baseline wander	33
4.2.4	Instrumental Noise	33
4.3	Pre-processing of ECG Signal using Wavelet transforms	36
4.3.1	Denoising ECG Signal using Discrete Wavelet Transforms	36
4.3.2	Baseline wander reduction of ECG Signal Using Discrete Wavelet Transforms	38
4.4	Conclusions	40
<b>Chapter 5</b>	<b>QRS COMPLEX DETECTION USING WAVELET TRANSFORMS</b>	<b>43</b>
5.1	Introduction	43
5.2	QRS detection algorithm	44
5.2.1	Algorithm based on Amplitude	

and First derivative	44
5.2.2 Algorithm based on First and Second derivatives	45
5.2.3 Digital filters	45
5.2.3.1 Okada algorithm	45
5.2.3.2 MOBD algorithm	46
5.2.4 Template matching techniques	46
5.2.4.1 Template cross correlation	46
5.2.4.2 Template subtraction	47
5.2.4 Discrete wavelet transform based technique	47
5.3 DWT – Based QRS detector	47
5.4 Conclusions	49
<b>Chapter 6 RESULTS AND DISCUSSION</b>	<b>51</b>
<b>Chapter 7 CONCLUSIONS AND FUTURE SCOPE OF THE WORK</b>	<b>57</b>
<b>REFERENCES</b>	<b>59</b>

---

## ABSTRACT

---

*Wavelet Transforms are widely preferred for the analysis of non-stationary signals because of their property of multi-resolution analysis, thereby implying the analysis of the signal of different frequencies with different resolutions. They are in turn robust to noise signals which are mixed up with the signal of interest during acquisition.*

*This report presents discrete wavelet transform based methods of pre-processing of the ECG signal for the removal of high frequency noise and low frequency baseline drift. It also presents a discrete wavelet transform based algorithm for the detection of QRS complex in the ECG signal. The algorithms have been tested using the CSE database.*

---

**INTRODUCTION**

---

**1.1 ELECTROCARDIOGRAM**

Electrocardiogram (ECG) is a graphic recording or display of the time-variant voltages produced by the myocardium during the cardiac cycle. ECG signal interprets heart action in terms of changing patterns of electrical potential on the human body. It is used clinically in diagnosing various cardiac diseases and conditions associated with the heart. Fig. 1.1 shows the waveform of the normal electrocardiogram. The P, QRS and T waves reflect the rhythmic electrical depolarization and repolarization of myocardium associated with the contractions of atria and ventricles. To the cardiologist, the shape and duration of each feature of the ECG are significant. In general, the cardiologist looks critically at the various time intervals, polarities and amplitudes to arrive at a proper diagnosis [1].

Under pathological conditions, several changes may occur in the ECG. These include (i) altered paths of excitation in the heart, (ii) changed origin of waves (ectopic beats), (iii) altered relationships (sequences) of features, (iv) changed magnitude of one or more features, and (v) differing durations of waves or intervals.

The number of cases of heart ailments among the masses has increased the workload of ECG analysis and diagnosis at an exponential rate. It has already crossed the limits of cardiologists to deal with all these



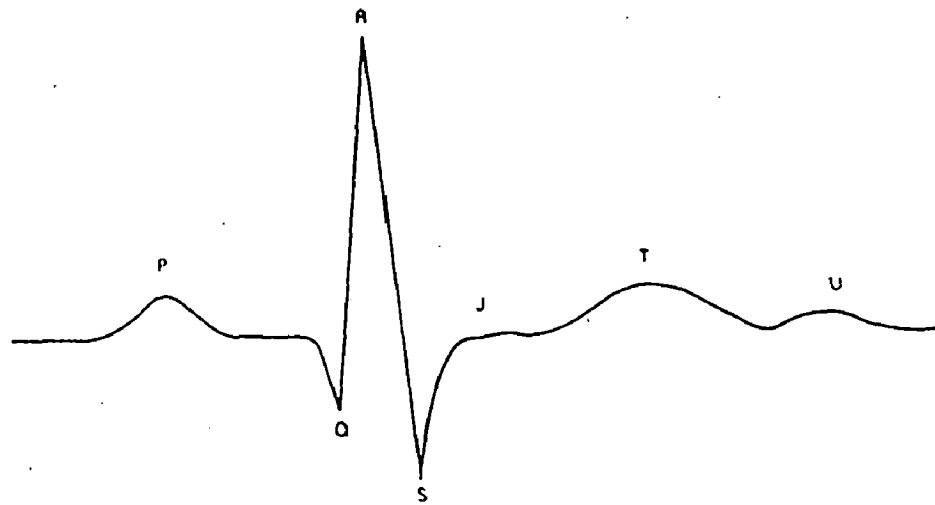


**Fig 1.1 The Electrocardiogram waveform.**

cases manually with utmost efficiency. Hence, the requirement of computer aided ECG analysis is indispensable. A good amount of work has been carried out in the past and lot of work is in progress for developing reliable techniques for fault free diagnosis of cardiac diseases.

QRS Complex detection in ECG signal is difficult, not only because of the physiological variability of the QRS complexes, but also due to various types of noises that can be present in the ECG signal, namely muscle noise, artifacts due to electrode motion, powerline interference and baseline wander [2].

Once the QRS complex is detected the other features of the ECG signal can be detected using different feature extraction methods of the signal [3]. In order to correctly extract the features, the ECG signal must be pre-processed to remove the noise contaminating the signal.

## **1.2 DISCRETE WAVELET TRANSFORMS**

Discrete wavelet transforms are reliable for the analysis of non-stationary signals such as ECG due to their multi-resolution capability [4]. The discrete wavelet transforms localizes the most important spatial and frequential features of a regular signal in a limited number of wavelet coefficients. They are very accurate and exhibits robustness to noise. They are in turn efficient for the removal of noise present in the signal [5].

## **1.3 ORGANIZATION OF DISSERTATION**

### **Chapter 1: Introduction**

This chapter deals in brief with the general introduction and the organization of the dissertation.

### **Chapter 2: Electrocardiogram**

In this chapter the general features of the ECG signal, various techniques of recordings of ECG signal and the noise associated with ECG are presented.

### **Chapter 3: Wavelet Transforms**

This chapter presents the general characteristics of Fourier Transforms and short time Fourier transforms and their disadvantages. It gives a brief introduction of wavelet transforms and their characteristic features.

### **Chapter 4: Pre-processing of ECG Signal**

In Chapter 4, a review about the various noise signals associated with the ECG and methods of their removal are presented. It also includes the pre-processing aspects of ECG signal using wavelet transforms.

## **Chapter 5: QRS complex detection using wavelet transforms**

A brief review of the various algorithms including the wavelet based QRS detector developed for QRS detection are presented in this chapter.

## **Chapter 6: Results and discussion**

This chapter includes the results of the three algorithms presented in Chapters 4 and 5. These algorithms use the discrete wavelet transform for pre-processing and QRS complex detection .

## **Chapter 7: Conclusions and future scope**

This chapter includes the conclusions drawn from the work carried out in this dissertation and also the scope for future work.

---

**ELECTROCARDIOGRAM**

---

**2.1 INTRODUCTION**

The biopotentials generated by the muscles of the heart result in the electrocardiogram. ECG has become a very popular and important tool next to stethoscope and blood pressure measuring instrument in the present time. The main advantage of ECG is its simplicity and noninvasive characteristics. The ECG provides faithful representation of the functioning of the heart.

**2.2 HEART PHYSIOLOGY AND FUNCTIONS**

The heart is one of the most critical organs of the human body. The function of the heart is rhythmic pumping of the blood that it receives from the veins and sends into the arteries. It is performed by alternate rhythmic contraction and relaxation of the muscular fibres which are the basic functional units of the muscular system [6].

The heart consists of several layers. The endocardium is the inner most layer which consists of smooth lining of the cells. Next to this is myocardium which constitutes the mass of the heart muscular cells. It is their coordinated contraction and relaxation that causes the chambers of the heart to pump the blood. The myocardium is covered by a layer of fat, called the epicardium. The pericardial sac which encloses the heart is formed by the outermost two layers of the pericardium which have a small amount of lubricating fluid between them. Although the heart consists of several layers,

it is only the myocardium that generates current large enough to be detected and recorded on the surface of the human body.

The heart consists of four chambers, namely the right and left atria, the right and left ventricles. The right atrium receives blood from different parts of the body which is oxygen deficient and rich in carbon dioxide through superior and inferior venacava. The blood is passed from right atrium to the right ventricle which pumps it out to the lungs for purification. The left atrium receives the purified oxygen rich blood from the lungs and passes it to the left ventricles which pumps it out to the circulatory network of the body through aorta, the network of arteries and capillaries. The valves located between these chambers are made in such a shape so that the blood flows only in one direction. This prevents the backward flow of blood when the blood filled chamber is contracted. The contraction of the myocardium of the chamber is known as the systole and the relaxation as the diastole.

### **2.3 FEATURES OF ECG SIGNAL**

ECG is a graphic recording or display of the time-variant voltages produced by the myocardium during the cardiac cycle [1]. Fig. 2.1 shows the basic waveform of the normal ECG.

The electrical activity during the cardiac cycle is characterized by five separate segments designated as P, Q, R, S and T waves.

**P-wave** : This is the deflection produced by the atrial depolarisation.

**Q-wave** : This is the initial negative deflection resulting from ventricular depolarisation.

**R-wave** : This is the positive deflection during ventricular depolarisation.

- S-wave** : This is the first negative deflection of ventricular depolarisation, that follows the first positive deflection (R).
- T-wave** : This is the deflection produced by ventricular repolarisation.
- U-wave** : This is present between T-wave and next P wave. It is a result of slow repolarisation of the intraventricular conduction.

The electrical potential and the corresponding frequency range and durations of these waves are given in Table 2.1.

**Table 2.1**

<b>Wave</b>	<b>Amplitude (mV)</b>	<b>Maximum frequency (Hz)</b>	<b>Duration (sec)</b>
P	0.25	10	0.20
R	1.6	20-30	0.45
Q	25% of R-wave	20-30	0.15
S	Upto 2	20-30	0.16
T	0.5	10	0.11

## **2.4 RECORDING OF ECG**

The amplitudes, polarities, event timing and duration of the ECG are dependent to a larger extent on the location of the electrodes on the human body.

To record ECG signal in 12 lead system, five electrodes are used which are fixed on the body of the patient. They are fixed on the following locations:

Right arm	-	RA
Left arm	-	LA
Right leg	-	RL
Left leg	-	LL
Chest	-	V <sub>1</sub> -V <sub>6</sub>

To record the ECG, following types of lead systems are used :

- (i) Bipolar standard limb leads
- (ii) Unipolar leads
- (iii) Unipolar chest leads or precordial leads
- (iv) Orthogonal leads

#### 2.4.1 Bipolar Standard Limb Leads

Figure 2.2(a) shows the placement of leads in bi-polar limb lead configuration. The three bipolar limb leads I, II and III are the original leads selected by Einthoven to record electric potential in the frontal plane.

The three bipolar limb leads first introduced by Einthoven are :

$$\text{Lead I} = \text{LA} - \text{RA}$$

$$\text{Lead II} = \text{LL} - \text{RA}$$

$$\text{Lead III} = \text{LL} - \text{LA}$$

RL is grounded and is called reference or ground lead.

In each of these lead positions, the QRS of a normal heart is such that the R wave is positive. Here, lead II produces the greatest R-wave potential.

#### 2.4.2 Unipolar Leads

The unipolar augmented limb leads are defined as follows :



$$\text{Lead aVR} = \text{RA} - \left[ \frac{\text{LL} + \text{LA}}{2} \right]$$

$$\text{Lead aVL} = \text{LA} - \left[ \frac{\text{RA} + \text{LL}}{2} \right]$$

$$\text{Lead aVF} = \text{LL} - \left[ \frac{\text{RA} + \text{LA}}{2} \right]$$

Fig. 2.2(b) shows the configuration of the placement of electrodes for unipolar leads aVR, aVL and aVF.

### 2.4.3 Unipolar Chest Leads or Precordial Leads

The leads  $V_1$  to  $V_6$  are unipolar leads located on the chest at different points, as shown in Fig. 2.2(c).

### 2.4.4 Orthogonal Leads

An ideal lead system for recording and Vector Cardiogram (VCG) essentially consists of the following characteristics:

- (i) The leads must be perpendicular to each other and also to the horizontal, vertical sagittal axis of the body.
- (ii) The amplitudes of the three leads should be equal from vectorial stand point.
- (iii) All the three leads should have the same strength and direction for all points in the heart where electromotive forces are generated. By convention, X, Y, Z are referred to as horizontal, vertical and sagittal axes and hence usually referred to as X, Y, Z leads [14].

The basic ECG lead configurations are shown in the Fig. 2.2.

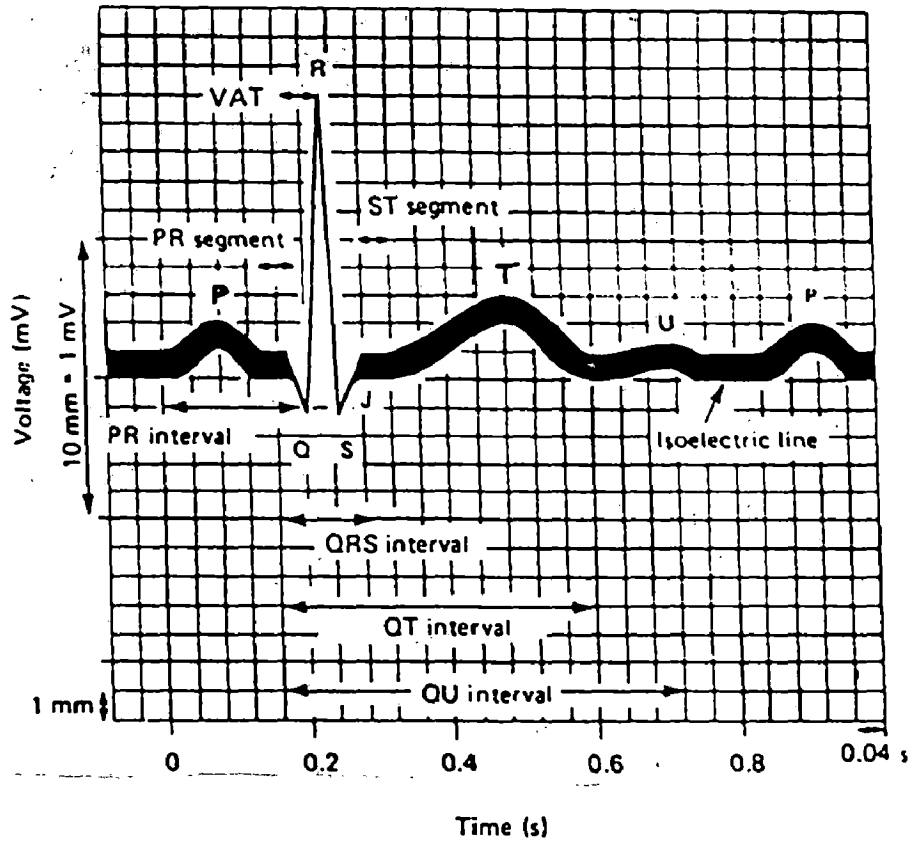
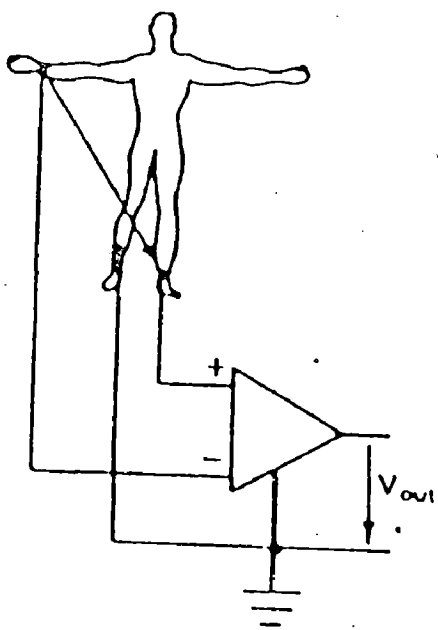


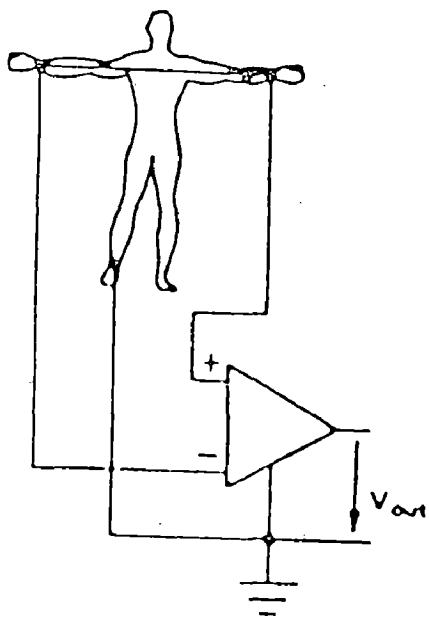
**Fig 2.1 Diagram of electrocardiographic complexes, intervals and segments [6].**

Bipolar limb leads

Lead II



Lead I



Lead III

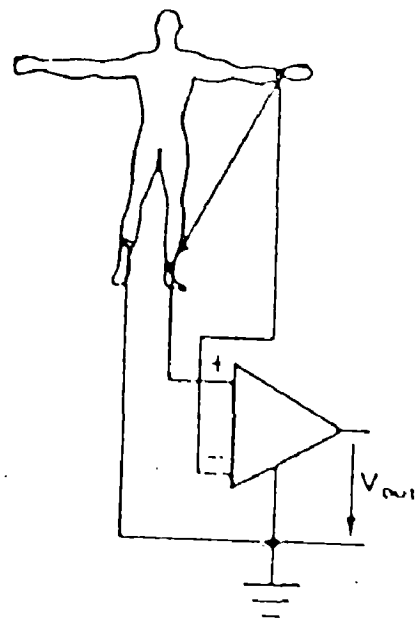
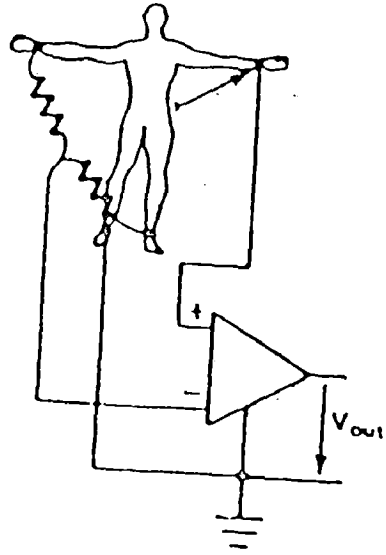


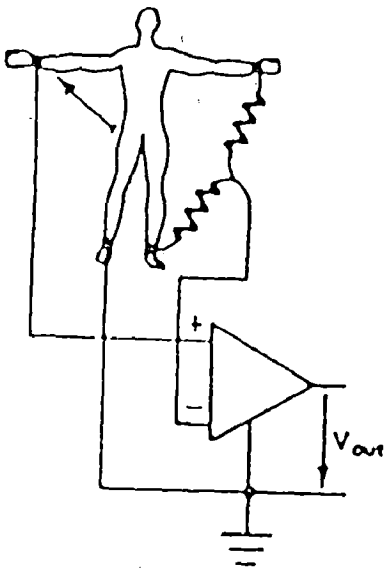
Fig 2.2(a) Bipolar limb leads

(Augmented) Unipolar limb leads

Lead aVL



Lead aVR



Lead aVF

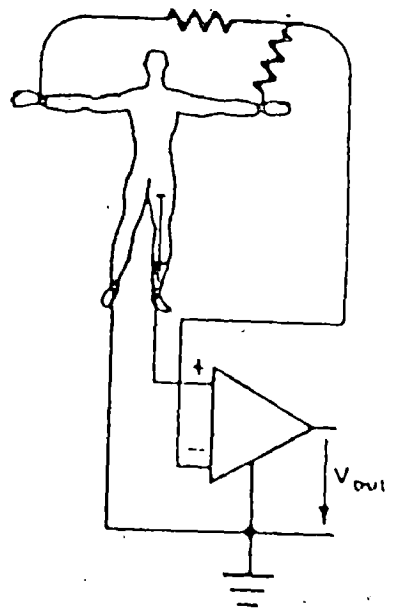
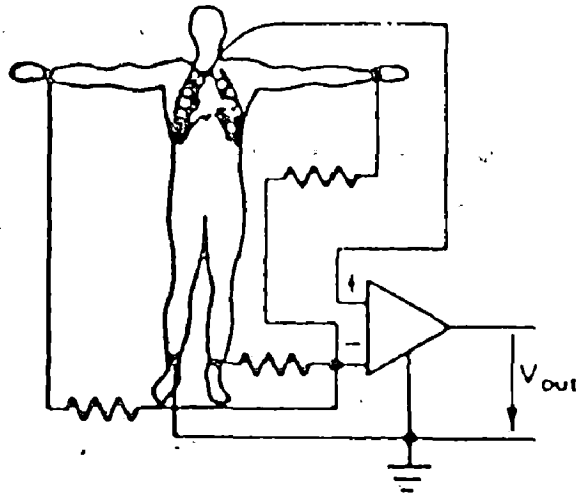


Fig 2.2(b) Unipolar limb lead (augmented)



- $V_1$  Fourth intercostal space, at right sternal margin.
- $V_2$  Fourth intercostal space, at left sternal margin.
- $V_3$  Midway between  $V_2$  and  $V_4$ .
- $V_4$  Fifth intercostal space, at mid-clavicular line.
- $V_5$  Same level as  $V_4$ , on anterior axillary line.
- $V_6$  Same level as  $V_4$ , on mid-axillary line.

Unipolar chest leads  
 $V_1 - V_6$

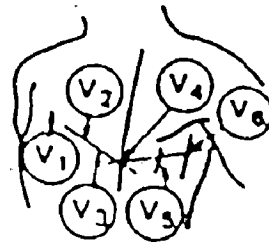


Fig 2.2(c) Precordial chest lead

## **2.5 NOISE ARTIFACTS IN ECG**

ECG signal may be corrupted by various kinds of noise. Typical examples are:

- (i) Power line interference.
- (ii) Electrode contact noise.
- (iii) Motion artifacts.
- (iv) Muscle contraction (Electromyographic).
- (v) Base-line drift and ECG amplitude modulation with respiration.
- (vi) Instrumental noise generated by electronic devices used in signal processing.
- (vii) Electrosurgical noise and other less significant noise sources.

A brief introduction of the noise in the ECG signal generated by the above sources and their methods of removal are presented in Chapter 4.

## **2.6 THE CSE DATABASE**

CSE stands for Common Standards for Quantitative Electrocardiography. The main objective for the development of CSE database was the standardization of ECG measurement procedures in quantitative terms, comparative studies of measurements performed by different programs and establishment of reference database for ECG measurements. CSE database consisted of five datasets. The datasets 1 and 2 consisted of 250 original and 310 artificial ECGs with 3-lead recording simultaneously. The datasets 3 and 4 consisted of 250 original and 250 artificial ECGs with 12-lead recording simultaneously. The dataset 5 was developed for diagnostic ECG. Here, the artificial ECG data was constructed by selecting one beat from each lead group of the original recordings and making strings of identical beats.

Here the CSE dataset -3 is considered since it is a measuring database with various onsets and offsets of the ECG signals. The CSE dataset 3 consists of 125 ECGs, with normal and different pathological ECGs. All ECGs were recorded at 500 Hz sampling frequency. The dataset consisted of 26% of normal cases and the remainder abnormal cases. Here, eleven leads were digitized simultaneously (that is, eight independent standard leads [I, II, V<sub>1</sub> to V<sub>6</sub>] and orthogonal leads X, Y and Z). The standard leads III, aVR, aVL and aVF were derived from leads I and II using the well known formulae [1]. Filtering or any other signal conditioning was not performed during data acquisition.

The dataset 3 had been tested by various programs which analyzed all the leads simultaneously or three or six or twelve at a time. Analysis had been done by various referees and the Median results of the referees coincided best with the median derived from all programs.

## **2.7 CONCLUSIONS**

As presented in this chapter, the ECG signal is a typical wave consisting of various waves designated as P, Q, R, S and T, in different frequency ranges with different amplitudes and durations (Table 2.1). Hence ECG signal is defined as a non-stationary signal since different frequency components exist at different time instants in a cycle. Generally, a signal is termed as a stationary one if its frequency content does not change with time.

---

**WAVELET TRANSFORMS**

---

**3.1 INTRODUCTION**

Wavelet transforms (WT) is a type of transformation which is capable of producing the time and frequency information simultaneously, hence giving the time-frequency representation of the signal. The wavelet transforms can localize both time and frequency components of the signal as the signal is processed at various scales [7]. Wavelet transforms are generally divided into two categories

- (i) Continuous wavelet transform (CWT)
- (ii) Discrete Wavelet Transform (DWT)

A brief introduction for the CWT and DWT is given in this chapter.

There are indeed other transforms like short time Fourier transforms, wigner distributions etc., but wavelet transforms are proved to be efficient regarding the resolution analysis.

The aim of signal analysis is to extract the relevant information from a signal by transforming it. The basic transform used for the analysis of frequency components of a signal is the Fourier transform.

**3.2 FOURIER TRANSFORM**

The Fourier transform decomposes a signal to complex exponential functions of different frequencies. The Fourier transform of a signal is given by the following equation



$$X(f) = \int_{-x}^x x(t).e^{-2j\pi ft} dt \quad (3.1)$$

where,  $t \rightarrow$  time

$f \rightarrow$  frequency

$x \rightarrow$  signal in time domain

$X \rightarrow$  signal in frequency domain, and

$e^{-t} \rightarrow \cos(t) - j\sin(t)$

As in equation (3.1), the signal  $x(t)$  is multiplied with the complex expressions of sines and cosines of frequency 'f'. If the signal has a high amplitude component of frequency 'f', then the component of the signal and the sinusoidal term will coincide and the product of them gives a relatively large value, otherwise not. Hence, Fourier transforms tells us whether a certain frequency component exists or not. It does not give any indication of the time at which the frequency component occurs. Hence, it is not suitable if the signal has varying frequency, i.e., when the signal is non-stationary. Since the ECG signal is a non-stationary signal as discussed in Chapter 1, the Fourier transform of it is not efficient because the time instance of the occurrence of frequency component is important for the analysis. Also, the ECG signal cannot be described by basis functions in terms of the sines and cosines easily with all its features covered faithfully [8].

In order to overcome this problem, the Short time Fourier transform are developed.

### 3.3 SHORT TIME FOURIER TRANSFORM (STFT)

The STFT of a signal is given by

$$\text{STFT}(\tau, f) = \int x(t) \cdot w^*(t - \tau) e^{-j2\pi ft} dt \quad (3.2)$$

where,  $w(t)$  is the window function and  $*$  is the complex conjugate. ' $\tau$ ' is the location of the window as the window is shifted through the signal.

Here the signal is divided into small enough segments, where these segments of the signal can be assumed to be stationary. Here, a window is selected whose length is equal to the segment of the signal where its stationarity is valid.

But STFT suffers from the lacuna that the window chosen is of finite length, thus covering only a portion of the signal, which causes the frequency resolution to get poorer, i.e., the exact frequency components that exist in the signal are not known. Indeed the time intervals in which certain band of frequencies exist can be known.

#### 3.3.1 Disadvantage of Short-Time Fourier Transforms

The resolution of the signal depends upon the selection of window length in case of STFT. Fig. 3.1 shows the difference lengths of windows for the gaussian window function in the form

$$w(t) = \exp(-a \cdot t^2 / 2)$$

'a' determines the length of the window.

Fig. 3.1(a) shows a narrow window. The STFT has a very good time resolution, but relatively poor frequency resolution.

Fig. 3.1(d) shows a wide window. The STFT has a good frequency resolution but relatively poor time resolution because, it covers a wide range of frequencies of the input signal.

Hence, if a narrow window is used, the time resolution of the signal is good and the frequency resolution is poor. If a wide window is used, the frequency resolution of the signal is good and the time resolution is poor.

Since ECG signal morphology changes from time to time, the selection of window of fixed length is not possible. Hence, if the STFT of the ECG signal is taken, a compromise must be made regarding the time resolution or the frequency resolution based on the selection of the window length.

In order to overcome the problem of resolution, wavelet transforms are proposed. Here, the length of window is not fixed and changes in accordance with the signal. As presented in the introduction to this chapter, there are two types of wavelet transforms i.e. continuous wavelet transforms and discrete wavelet transforms.

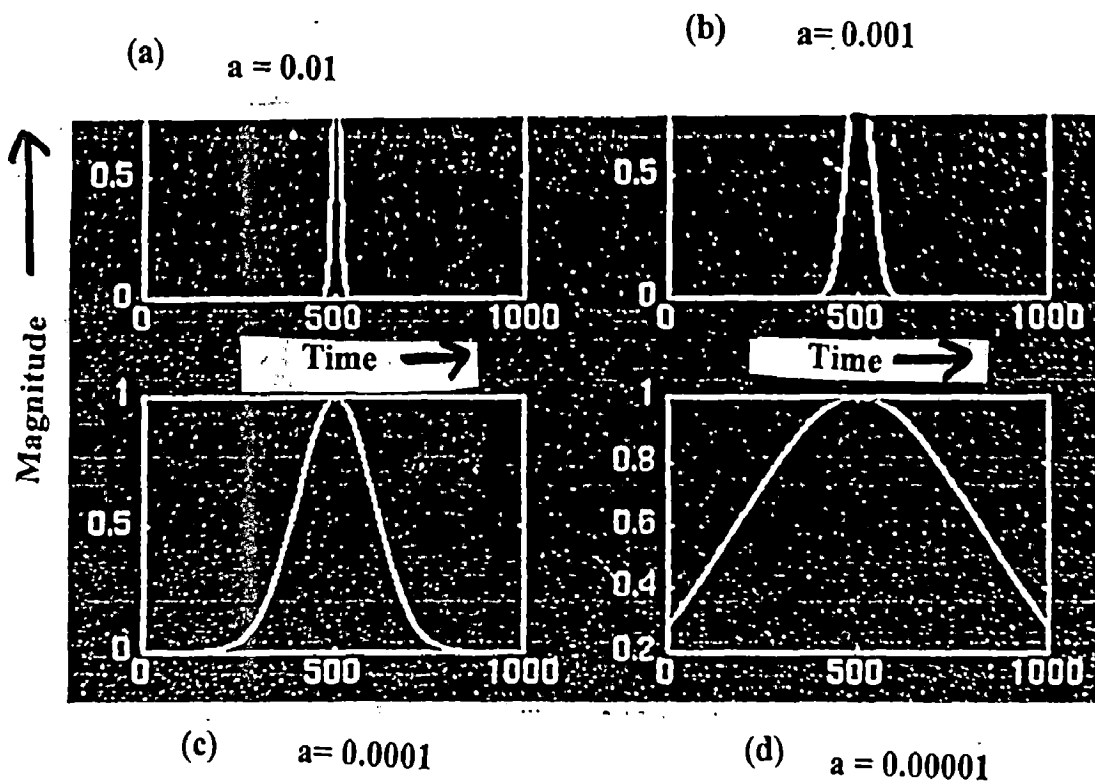


Fig 3.1 Gaussian window function of varying regions of support[4].

- (a)  $a = 0.01$
- (b)  $a = 0.001$
- (c)  $a = 0.0001$
- (d)  $a = 0.00001$

### 3.4 CONTINUOUS WAVELET TRANSFORMS (CWT)

The continuous wavelet transforms was developed as an alternative approach to the STFT to overcome the resolution problem.

The continuous wavelet transform is defined as

$$\text{CWT}(\tau, s) = \frac{1}{\sqrt{|s|}} \int x(t) \cdot \psi \left( \frac{t - \tau}{s} \right) dt \quad (3.3)$$

As seen from the equation 3.3, the transformed signal has two variables, ' $\tau$ ' and ' $s$ '. ' $\psi(t)$ ' is the transforming function, called mother wavelet. The mother wavelet serves as a prototype for generating the other window functions. The variables ' $\tau$ ' and ' $s$ ' are named as 'translation' and 'scale' parameters respectively.

The term 'translation' refers to the location of the window, as the window is shifted through the signal. The term scale has an important significance. Here, high scales correspond to the global information of a signal (that usually spans the entire signal) whereas low scales correspond to a detailed information of a hidden pattern in the signal (that usually lasts a relatively short time), i.e., large scales dilates the signal and small scales compress the signal. In wavelet transform, the scales  $s > 1$  dilates the signals whereas scales  $s < 1$  compresses the signal.

Since mother wavelet is chosen to serve as a prototype for all windows, all the windows used are the dilated (or compressed) and shifted versions of the mother wavelet [7].

Fig.3.2 shows the interpretation of the time and frequency resolutions. Here, each box corresponds to a value of the wavelet transform in the time-frequency plane. Although the widths and heights of the boxes change, the

area is constant. Hence, we see that each box represents an equal portion of the time-frequency plane with respect to area, but giving different proportions to time and frequency with time and frequency taken independently. We see that at low frequencies, the height of the boxes w.r.t. y-axis are shorter (which corresponds to better frequency resolution, since there is less ambiguity regarding the value of exact frequency), but their widths w.r.t. x-axis are longer (which corresponds to poor time resolution, since there is more ambiguity regarding the value of the exact time). At higher frequencies, the width of the boxes decreases, i.e., the time resolution gets better and the height of the boxes increases, i.e., the frequency resolution gets poorer.

From the CWT, if the signal has a spectral component that corresponds to the current value of 's', the product of the wavelet with the signal of the location where this spectral component exists gives a relatively large value. If the spectral component that corresponds to the current value of 's' is not present in the signal, the product value will be relatively small. Here WT have the property to analyze the signal using Multi Resolution Analysis (MRA) [4]. The MRA implies that the analysis of the signal is made at different frequencies with different resolution.

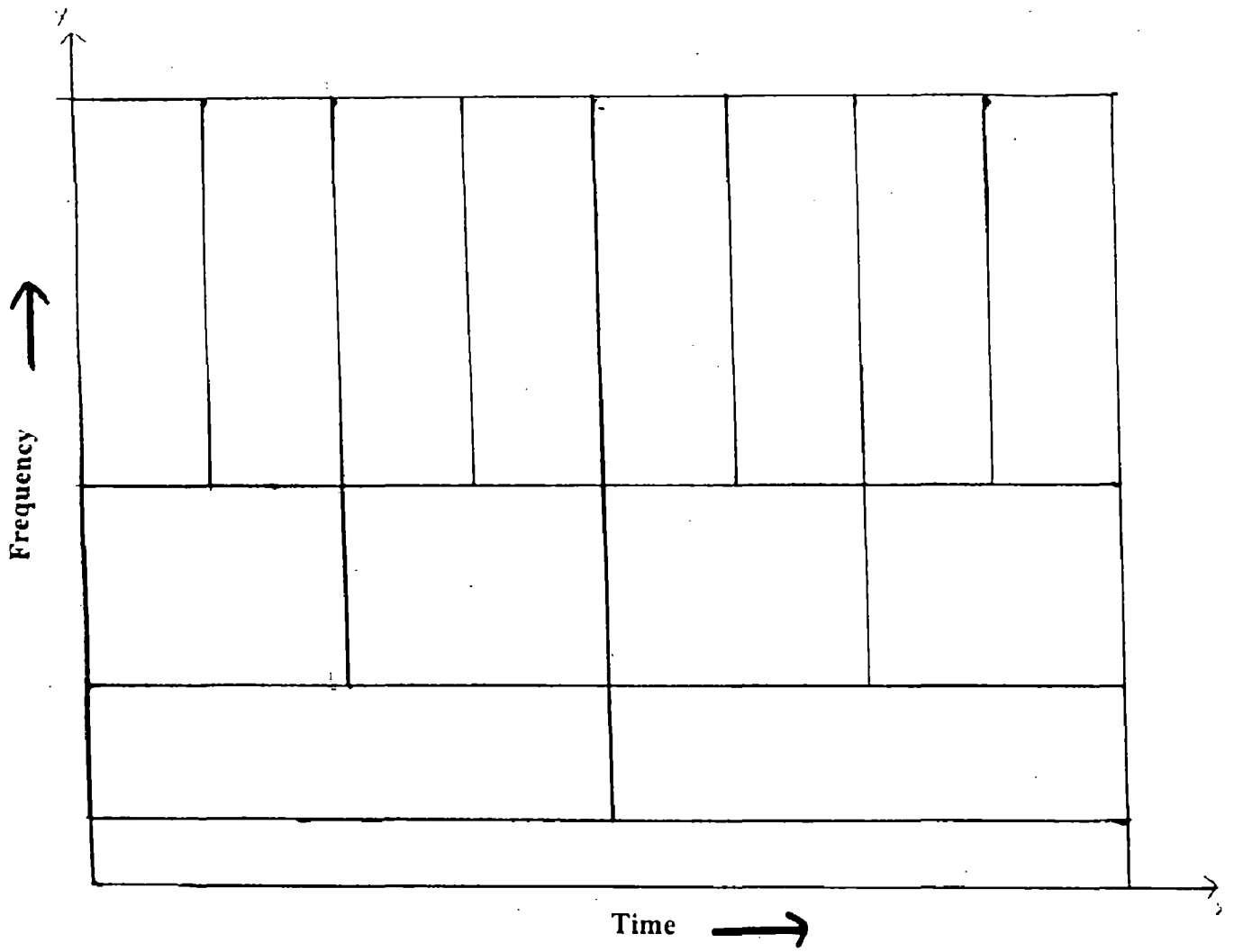


Fig 3.2 Time and Frequency resolutions

ALL BOXES HAVE EQUAL AREA

The main disadvantages of CWT are computational complexity and redundancy. Hence discretized CWT are developed by discretizing either ' $\tau$ ' or 's' or both. Here the parameter 's' is discretized first on a logarithmic grid. The time parameter is then discretized with respect to the scale parameter, i.e., a different sampling rate is used for every scale. But this process creates a high redundancy as far as the signal re-construction is concerned [4]. So, the discrete wavelet transforms are developed in order to overcome the problem of redundancy associated with continuous wavelet transform, which significantly reduces the computation time.

### **3.5 DISCRETE WAVELET TRANSFORM (DWT)**

The DWT are easier to implement than CWT. The DWT is based on the process of Subband Coding.

The CWT is computed by changing the scale of the analysis, shifting the window in time, multiplying by the signal and integrating over all times as presented in section 3.4. In discrete wavelet transform, filters of different cutoff frequencies are used to analyze the signal at different scales. The signal is passed through a series of high pass filters to analyze the high frequencies and through a series of low pass filters to analyze the low frequencies.

Filtering of a signal in discrete time corresponds to the mathematical operation of convolution of the signal with the impulse response of the filter.



The convolution operation in discrete time is defined as

$$x[n] * h[n] = \sum_{k=-\infty}^{\infty} x[k].h[n - k] \quad (3.4)$$

where  $h[n] \rightarrow$  Low pass filter

$x(n) \rightarrow$  Input signal

$$x[n] * g[n] = \sum_{k=-\infty}^{\infty} x[k].g[n - k] \quad (3.5)$$

where,  $g(n) \rightarrow$  High pass filter.

The discrete wavelet transform is implemented in the form of sub-band coding. The Subband Coding algorithm is shown in Fig. 3.3.

The original signal is convolved with high pass filter, according to the equation (3.4). Similarly the original signal is convolved with the low pass filter and half of the samples are eliminated according to the Nyquist's rule. Here the signal is subsampled by 2.

Here, the high pass filter removes all frequencies that are below half of the highest frequency in the signal. Similarly, the low pass filter removes all the frequencies that are above half of the highest frequency in the signal.

Discarding every other sample, subsamples the signal by two. Here, low pass filtering removes the high frequency information thereby altering the resolution. Subsampling process changes the scale. Here, the time resolution of the signal is halved after each filter operation.

As shown in Fig. 3.3, first the signal is passed through high pass filter. The output of high pass filter after sub sampling corresponds to the detailed information of the input signal in the range  $\pi/2 \sim \pi$  radians. Similarly, the input signal is passed through the low pass filter. Now half of the samples

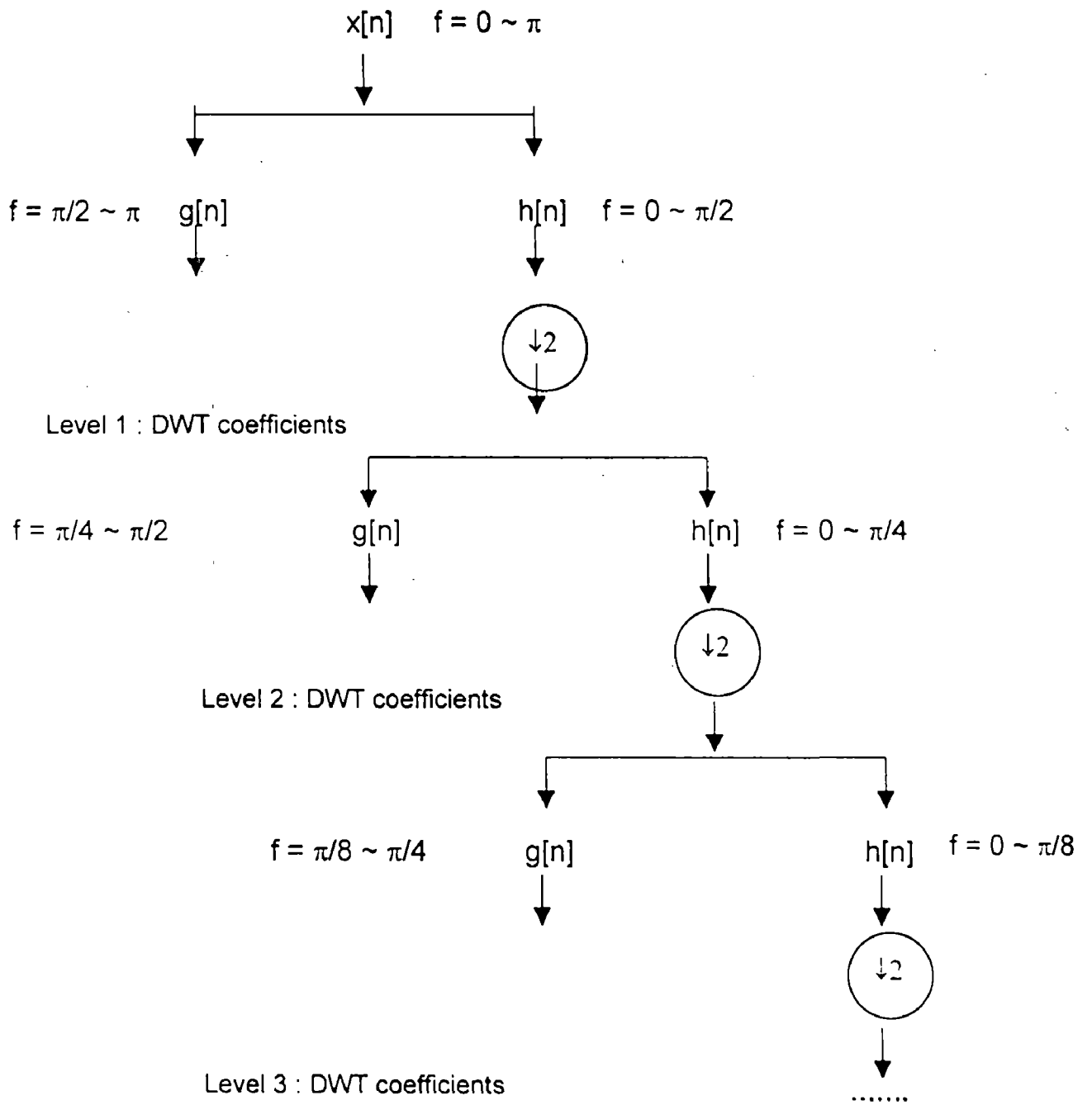
are eliminated, since the signal has the highest frequency of  $\pi/2$  radians, according to Nyquist criteria [4]. The signal obtained at the output of low pass filter is the approximation signal. Here, the detail signal corresponds to the output of the high pass filter. The detailed level is the level 1 DWT coefficients of Fig.3.3 which corresponds to the high frequency components of the input signal. This process is repeated for the next lower level until the desired frequency range is achieved.

Here the frequencies that are most prominent in the original signal will appear as high amplitudes in that region of the DWT signal that includes those particular frequencies. Here, the localization of these frequencies is preserved. If the main information of the signal lies in the high frequencies, the time localization of these frequencies will be more precise since these are characterized by more number of samples. Here, this process has good time resolution at high frequencies and good frequency resolution at low frequencies.

The high pass and low pass filters are not independent of each other and are related by  $g [ L - 1 - n ] = (-1)^n.h[n]$

Where  $L =$  length of the filter.

As an example, if the input signal is sampled at 500 Hz sampling frequency, the implementation of the DWT algorithm for this signal at different levels of decomposition is shown in Fig. 3.4.



$x[n]$  = Original signal  
 $g[n]$  = High pass filter  
 $h[n]$  = Low pass filter

**Fig. 3.3 : Subband Coding Algorithm**



Some of the wavelets used for the analysis are given in the Table 3.1[9].

Table 3.1

Wavelet	Low pass filter coefficients h(n)	High pass filter coefficients g(n)
<b>Daubechies</b>		
4	0.482962, 0.836516, 0.224144, -0.129409	$g(L-1-n) = (-1)^n$ h(n) L = length of filter
6	0.33267, 0.806891, 0.458775, -.135011, -0.085441	-do-
8	0.230378, 0.714846, 0.630881, -0.27984, -0.187034, 0.030841, 0.032883, -0.010597	-do-
10	0.160102, 0.603829, 0.724308, 0.138428, -0.242294, -0.03224, 0.077571, -0.006241, -0.012581, 0.003336	-do-
<b>B-Spline</b>	0.5, 0.25, 0.5	-do-
<b>Type</b>		
Linear		
Cubic	0.0625, 0.25, 0.375, 0.25, 0.0625	-do-
Quadratic	0.125, 0.375, 0.375, 0.125	-2.0, 2.0

### **3.6 CONCLUSIONS**

From the above presentation on wavelet transforms, it is seen that wavelet transform is most suited for the analysis of non-stationary signals such as ECG since it has the capacity to analyse the signal at different frequencies with different resolutions.

---

**PRE-PROCESSING OF ECG SIGNAL**

---

**4.1 INTRODUCTION**

The ECG signal is corrupted by various sources of noise. The feature extractions from the ECG signal can be made more accurate if the input ECG signal to the processing system is made free from the noises associated with it.

**4.2 SOURCES OF NOISE**

While recording the ECG, unwanted signals interfere with it and hence ECG signal gets corrupted with noise. Typically the noise sources are classified as:

- (1) Power line interference.
- (2) Muscle artifacts.
- (3) Baseline wander.
- (4) Instrumental noise.

**4.2.1 Power Line Interference**

The inductive coupling is from neighbouring power frequency devices by magnetic flux linking with the lead wire from the patient to the ECG machine. It may be reduced by twisting the lead wire in a systematic fashion so as to reduce the effective area of flux linking. The capacitive coupling from the power frequency device is due to the lead wire as well as to the patient. The method of completely eliminating power frequency interference

is to provide effective shielding to the patient and the machine. This interference produces 50 Hz signal, which is as shown in Fig. 4.1(a).

#### **4.2.2 Muscle Artifacts**

Whenever a muscle is activated, it produces an EMG signal. The electrodes, placed at this site, pick up the unwanted EMG signal. This causes abrupt variations of voltages. Hence a high frequency noise is produced with a frequency range of dc to 10000 Hz and peak amplitudes varying from 50  $\mu$ V to about 1 mV. The ECG corrupted with EMG noise is shown in Fig. 4.1(c). The signals resulting from muscle contraction can be assumed to be transient bursty of zero-mean band limited Gaussian noise. Gaussian noise is the noise which spans over the entire frequency range of the signal. Theoretically, the Gaussian white noise is assumed to be of infinite bandwidth.

#### **4.2.3 Baseline Wander**

If the electrode contact is not proper or if there is a body movement, the baseline wanders or drifts. This introduces low frequency noise of the order of 0.5Hz. The baseline also drifts with respiration which can be represented as a sinusoidal component at the frequency of respiration added to the ECG signal as shown in Fig. 4.1(c).

#### **4.2.4 Instrumental Noise**

This is generated within the recording instrument which causes high frequency periodic variations in the ECG signal. Artifacts generated by electronic devices in the instrumentation system as shown in Fig. 4.1(d) can



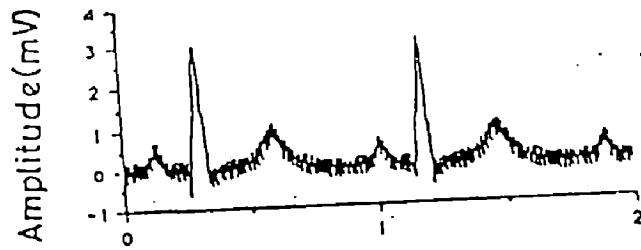
not be corrected by QRS detection algorithm. Here, the input amplifier is saturated and no information about the ECG signal can reach the detector. Here an alarm must sound to alert the ECG technician to take corrective action. While recording ECG, the signal is corrupted by both high frequency and low frequency noises.

The best performance of an ECG processing system is achieved if the input signal is free from noise. The removal of noise is important not only for computer processing but also for visual examination of the ECG waveform. Several filters have been designed to pre-process the ECG signal for the removal of noise content present in it [10,11]. A few filters are discussed below.

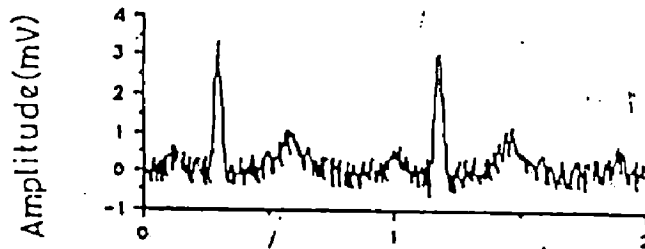
Finite impulse response (FIR) filters are normally preferred for noise removal from the ECG as they introduce minimum signal distortion because of their linear phase characteristics.

A multi band filter known as extraction filter which uses integer arithmetic is designed and implemented for the removal of baseline drift and powerline interference in the ECG signal [11]. This filter is designed for real time execution.

An other online digital filter developed for the subtraction of 50 Hz interference from the ECG signal used the postulate that the interference can be measured in intervals of the ECG signal, where the latter is isoelectric or changes linearly with time. The sum of equally spaced sample amplitudes from one period of a periodic interference signal is zero. The interference of the signal is reduced based on the criteria of threshold selection derived from the backward differences [12]. The above algorithms work for removal of 50 Hz signal only.



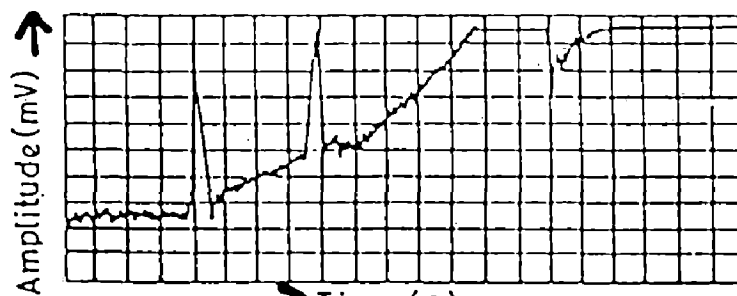
→ Time  
(a).



→ Time  
(b)



→ Time  
(c)



→ Time (s)  
(d)

Fig 4.1 ECG with noise [2]

- (a) Power line interference
- (b) Electromyographic noise
- (c) Base line drift due to respiration
- (d) Instrumentation saturation

The wavelet based noise reduction is effective in the removal of the Gaussian noise present in the ECG signal and also the 50 Hz interference signal. Since the ECG signal has the frequency range of 0-30 Hz generally and the high frequency noise has the range that does not overlap with that of the ECG signal, the noise is well isolated from the ECG signal.

#### **4.3 PRE-PROCESSING OF ECG SIGNAL USING WAVELET TRANSFORMS**

Here, two different algorithms are implemented using discrete wavelet transforms to pre-process the ECG signal, one for the removal of high frequency noise present in the signal due to soft tissue motion artifacts and the other for the reduction of baseline drift present in the ECG signal.

##### **4.3.1 Denoising ECG Signal Using Discrete Wavelet Transforms**

Here, an off-line denoising algorithm is implemented based on adaptive wavelet technique. Wavelet-based noise removal exploits the time/scale characteristic of the DWT. Normally, noise consists of high-frequency components and is thus localized in the finer, detailed levels of the DWT. In these levels, the important coefficients, corresponding to the true signal information, have a relatively high magnitude, and the lower magnitude coefficients represent the noise. The expected noise energy is the same in all coefficients. Hence if this energy is not too large, noise has a relatively small influence on the important large signal coefficients. Therefore the small coefficients should be replaced by zero, because they are dominated by noise and carry only small amount of information.

Here, the variable white noise (Gaussian noise) is added to the ECG signal to produce the noisy output. Here, the signal is decomposed using Daubechies wavelet-6 (Table 3.1). At each level of decomposition, the standard deviation( $\sigma_i$ ) of the wavelet coefficients is calculated and then the threshold is defined based on the value ' $\alpha_i \cdot \sigma_i$ ' where ' $\alpha_i$ ' is a variable. Here, three levels of decomposition are chosen for the high frequency noise removal of the ECG signal. Since the noise corresponds to high frequency contents of the signal, at the finest or detailed scale, ' $\alpha_i$ ' is set to a relatively large value to remove the noise components present at that level. Then at the next lower levels  $\alpha_i$  is reduced and the process is repeated. The values of ' $\alpha_i$ ' for the three levels are presented in Chapter 6. This process is repeated for three levels of decomposition considered and then the reconstruction of the signal is made. The root mean square error (RMSE) and the percent root mean square difference (PRD) of the actual signal without noise and the reconstructed signal is calculated to judge the performance of the algorithm.

The root mean square error is defined as

$$\text{RMSE} = \sqrt{\frac{1}{N} \sum_{i=1}^N [x_{\text{org}}(i) - x_{\text{rec}}(i)]^2}$$

where  $x_{\text{org}}(i) \rightarrow$  original input signal

$x_{\text{rec}}(i) \rightarrow$  reconstructed signal

and  $N \rightarrow$  total number of samples

and the percent root mean square difference is defined as

$$\text{PRD} = \left[ \frac{\sum_{i=1}^N [x_{\text{org}}(i) - x_{\text{rec}}(i)]^2}{\sum_{i=1}^N [x_{\text{org}}(i)]^2} \right]$$

The general algorithm for denoising ECG signal is presented on page no. 39.

#### **4.3.2 Baseline Wander Reduction of ECG Signal Using Discrete Wavelet Transforms**

Here also, an off-line algorithm is implemented to reduce the baseline drift of the ECG signal. Generally, the baseline wandering can make the inspection of the ECG signal difficult because some features can be masked by it. More over, in automatic inspection systems, the other processing tasks such as wave detection, signal classification, etc., can be affected.

As presented in Chapter 3, at each level of decomposition of the DWT, the input signal is decomposed into two parts, i.e. detail or high frequency components, and the approximation itself or the low frequency components. Here, the approximation of the signal is considered for the reduction of baseline drift in ECG signal since the approximation signal and baseline drift are low frequency signals.

The best level of approximation of the signal is decided based on measure of the resulting signal variance at that level. In order to reduce the baseline wandering, the approximation found must have a narrow spectrum and the variance of the resulting signal should be as low as possible, since the approximation must not have high frequency components of the signal.

Here, the input signal is sampled at 500Hz sampling frequency, and hence the eighth level of approximation corresponds to the frequency range of (0-1)Hz which is the frequency range of the baseline wandering. The eighth level of approximation is calculated, and then, it is subtracted from the signal. Consequently, the baseline wander of the signal is greatly reduced.

For the purpose of testing this algorithm, a sinusoidal signal is generated with the sampling frequency of 500 Hz and the low frequency signal of 1 Hz is added to it. The algorithm is tested on this signal and it is seen that the eighth level of decomposition corresponds to the low frequency component of 1 Hz and the corresponding low frequency component is effectively reduced by subtracting it from the original signal.

The general algorithm for the baseline wander reduction is presented on page no. 40.

The codes are developed in 'C' language for the implementation of the two algorithms. The results of the two programs are presented in chapter 6.

#### ALGORITHM FOR DENOISING OF ECG SIGNAL

1. Input the ECG signal data file.
2. Calculate the DWT of the signal at the scale  $S=2^i$ ,  $i=1$ , the array  $b[j]$  contains the coefficients of the detail level or the output of high pass filter.
3. Calculate the standard deviation ( $\sigma_i$ ) of the detail signal at this level.
4. Calculate ' $\alpha_i \cdot \sigma_i$ ' for  $i = 1$  and make  $b[j]=0$  for  $b[j] < (\alpha_i \cdot \sigma_i)$ . [ $\alpha_i = 2.0, 1.5, 0.5$  for  $i = 1, 2, 3$  respectively.]

5. For  $i=2$ , repeat steps 2, 3 and 4.
6. For  $i=3$ , repeat steps 2, 3 and 4.
7. Reconstruct the signal starting from the lowest level ( $i=3$ ) by up-sampling and then convolving the high pass and low pass filters.
8. Calculate the RMSE and PRD.

#### **ALGORITHM FOR BASELINE WANDER REDUCTION**

1. Input the ECG signal.
2. Calculate the DWT of the input signal at scales  $S=2^i$ ,  $i= 1$  to 8.
3. Interpolate the eighth level of approximation signal linearly to get the samples corresponding to the input signal.
4. Subtract the input signal from the coefficients obtained after interpolation.

The flowcharts of the two algorithms discussed are given in Fig. 4.2 and Fig. 4.3.

#### **4.4 CONCLUSIONS**

Here, two algorithms based on the Discrete Wavelet Transforms for the reduction of high frequency and low frequency noise in the ECG signal have been presented. It is seen that the algorithm for baseline wander reduction works effectively for the testing sinusoidal signal, with the low frequency component added to it. The low frequency signal is separated from the sinusoidal signal and thus it is reduced as per the algorithm.

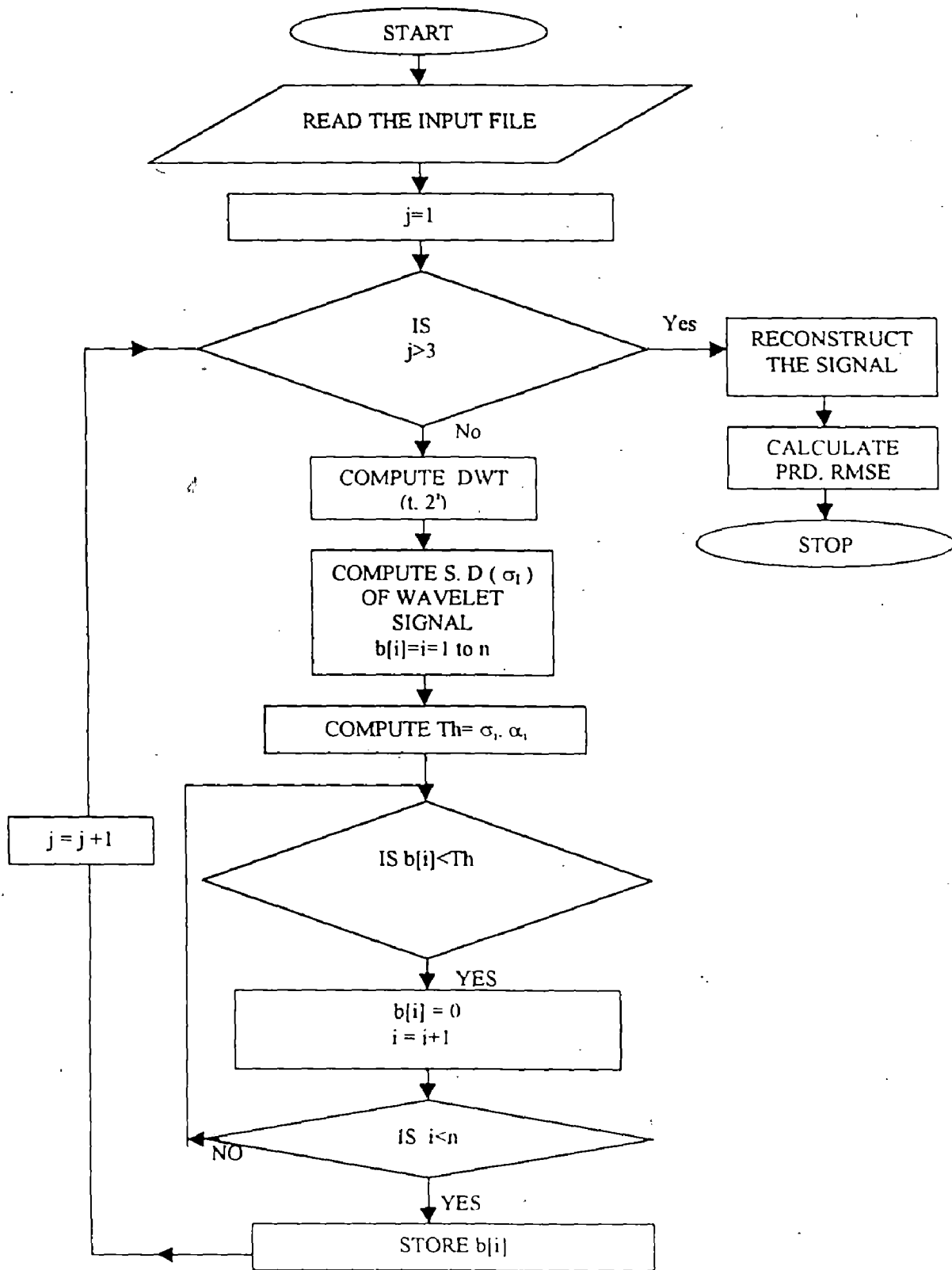


Fig 4.2 Flow Chart for Denoising of ECG Signal



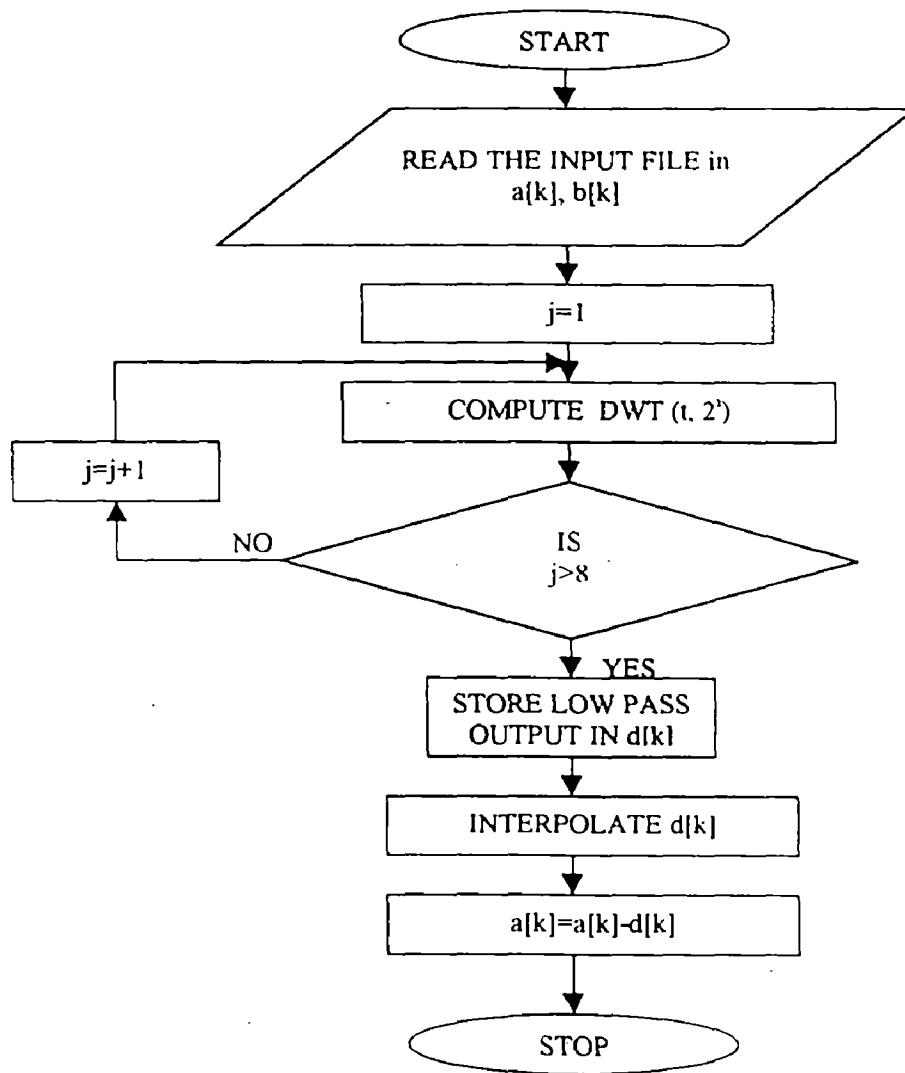


Fig 4.3 Flow Chart for Baseline Wander Reduction

## **QRS COMPLEX DETECTION USING WAVELET TRANSFORMS**

---

### **5.1 INTRODUCTION**

The detection of QRS complex – specifically, the detection of the peak of the QRS complex or R wave in an ECG signal is a difficult problem since it has a time-varying morphology and is subject to physiological variations due to the patient and due to corruption with noise. Since the QRS complexes have a time-varying morphology, they are not always the strongest signal component in the ECG signal. Therefore P-wave or T-wave with characteristics similar to that of QRS complex, as well as spikes from high frequency pacemakers can compromise the detection of QRS complex. In addition, there are many sources of noise in a clinical environment that can degrade the ECG signal. These include powerline interference, muscle contraction noise, poor electrode contact, patient movement and baseline wander due to respiration. Therefore QRS detectors must be invariant to different noise sources and should be able to detect QRS complexes even when the morphology of ECG signal is varying with time.

Most of the current QRS detectors can be divided into two stages: a preprocessor stage to emphasize the QRS complex and a decision stage to threshold the QRS enhanced signal. In the preprocessor stage, the ECG signal is first bandpass filtered to reduce noise and differentiated to emphasize the large slope of the R-wave and then squared to further exploit the high-frequency content of the QRS complex. A short time energy estimate is obtained by smoothing the resulting signal with a moving

window integration. The selection of bandwidth of the bandpass filter and the duration of the sliding analysis window is not straightforward. The bandwidth of the bandpass filter must be chosen to reflect the trade-off between noise reduction and loss of high-frequency details. If the bandwidth is too large, noise reduction suffers. If the bandwidth is too small, high frequency QRS characteristics are lost. Similarly a long window allows a large energy accumulation whereas a short window allows too little energy to accumulate. So a fixed bandwidth of bandpass filter and fixed window length can not serve the purpose of detection of QRS complex in ECG signal.

A number of algorithms have been proposed for the ECG QRS detection, These include the algorithms based on amplitude and first derivative, based on first and second derivative, based on digital filters [3] but each algorithm has its own advantages and disadvantage.

## **5.2 QRS Detection Algorithms**

The performance of any QRS detection algorithm depends on the accurate detection of QRS complex in the presence of noise.

### **5.2.1 Algorithm based on amplitude and first derivative**

In this algorithm, the largest positive valued element of the array containing the ECG data points is calculated and is taken as a reference for the threshold [3]. The first derivative  $y(n)$  is calculated at each point of input signal  $x(n)$  such that

$$y(n) = x(n+1) - x(n-1) \quad 1 < n < N,$$

where 'N' is the total number of samples.

A QRS complex occurs when three consecutive points in the first derivative array exceed a positive slope threshold and are followed within the next 100 ms by two consecutive points which exceed the negative (descending slope) threshold [3].

### **5.2.2 Algorithm based on first and second derivatives**

Here, the absolute values of the first and second derivatives are calculated from the ECG, the scaled sum of the first and second derivatives is stored and scanned until the threshold is met or exceeded [3]. Once this occurs, the next eight points are compared with the threshold. If six or more of these eight points exceed the threshold, the QRS complex is identified.

The above two algorithms do not work satisfactorily because QRS complex has a time varying morphology and can not be judged with the slope criteria alone.

### **5.2.3 Digital Filters**

Two algorithms based on the digital filters for QRS detection are presented below.

#### **5.2.3.1 Okada Algorithm**

This algorithm is proposed by Okada [13]. Here the smoothing of input signal is made by three point moving average filter, and is passed through the low pass filter. It effectively reduces a band pass filtering operation on the original data. The difference signal is then squared. To further highlight the high frequency QRS complex, the resulting signal is multiplied by a non-linearly filtered version of itself.

### **5.2.3.2 MOBD Algorithm**

This algorithm proposed by Suppappola and Sun, referred to as multiplication of the backward differences(MOBD), used only non-linear filtering to detect the QRS complex. Here, to emphasize the high frequency characteristics of the signal, the square of the derivative (or backward difference) of the signal is calculated. The successive samples of the backward difference of the ECG signal are multiplied together to highlight the high frequency content of the signal [15].

As seen from the above two algorithms, their implementation involve complex programming. Moreover the QRS complexes are suppressed along with the noise by these algorithms [3]. The best performance of the above algorithms is achieved when the signal is first pre-processed for the removal of various noise components associated with it.

The advantage of using Discrete Wavelet Transforms over the above algorithms described for QRS detection includes the easy implementation of DWT algorithm, which does not require any pre-processing stage for the noise reduction before the detection of QRS complex.

### **5.2.4 Template Matching Techniques**

In these methods, templates are used for classifying the patterns in the ECG signal that are quite related to the human recognition process.

#### **5.2.4.1 Template Cross Correlation**

Here the template of a QRS waveform is correlated with the incoming ECG signal and the value of the cross-correlation coefficient is calculated. If the coefficient is high, then it is identified as a QRS complex [15].

#### **5.2.4.2 Template subtraction**

Here also the template of the QRS waveform is stored and is compared with the incoming ECG signal. Each point of the incoming signal is subtracted from the corresponding point in the template. The QRS complex is decided by the low value of the resulting subtraction [15]. Other techniques include automata-based template matching where the ECG signal is reduced to a set of pre-defined tokens[15].

In the template matching technique discussed, the selection of a template is difficult because QRS complex has different shapes for different leads and also all the peaks in the QRS complex (Q, R and S) are not always present which makes the matching difficult.

#### **5.2.5 Discrete Wavelet Transform Based Technique**

Here a discrete wavelet transform (DWT) is used to overcome the above problems. A chosen "mother wavelet" has a fixed shape, however the wavelet derived from it by changing scales, referred to as "daughter" wavelets, have different bandwidths and time supports. At any particular scale, the DWT is the convolution of the signal and the time-scaled daughter wavelet. Scaling the mother wavelet is the mechanism by which the DWT adapts to the spectral and temporal changes in the signal being analyzed. So, for smaller scale values, it exhibits high temporal and low spectral resolution whereas for larger scale values, it exhibits low temporal and high spectral resolution.

### **5.3 DWT – BASED QRS DETECTOR**

As most of the energy distribution of QRS complex lies in the range of 6-30 Hz [14], it is taken as a reference for wavelet based QRS detector as

the frequency range specified above lies in the fourth level of decomposition and the QRS detection is performed at fourth level itself. However, since QRS complex is a transient and the DWT computed exhibits local maxima across several scales at the instance of occurrence of transients [14], the fourth and the successive levels are taken as reference to ascertain the QRS peak. Here the ECG signal is sampled at 500 Hz.

*The algorithm is as follows:*

1. Read the input data file
2. Compute the DWT of the input signal at scales  $S = 2^i$ ,  
 $i = 1$  to 5.
3. Store the detailed signal at fourth and fifth levels.
4. Locate the local maxima across the two levels which exceed a threshold Value.
5. If the corresponding local maxima across the two levels lies within the range of  $\pm 15$  samples, go to 6 else go to 7.
6. Store the corresponding data point at fourth level. Advance the search to fifteen data points ahead. Go to 5.
7. Ignore that sample, move to the next one and go to 5.
8. Output the QRS peaks.

Here, two wavelets are taken and the analysis is made for different filter lengths. The algorithm is tested with CSE database. The two wavelets used are Quadratic spline wavelet and Daubechies wavelet-10 (table 3.1). The two wavelets are first tested on the known sinusoidal signal of sampling

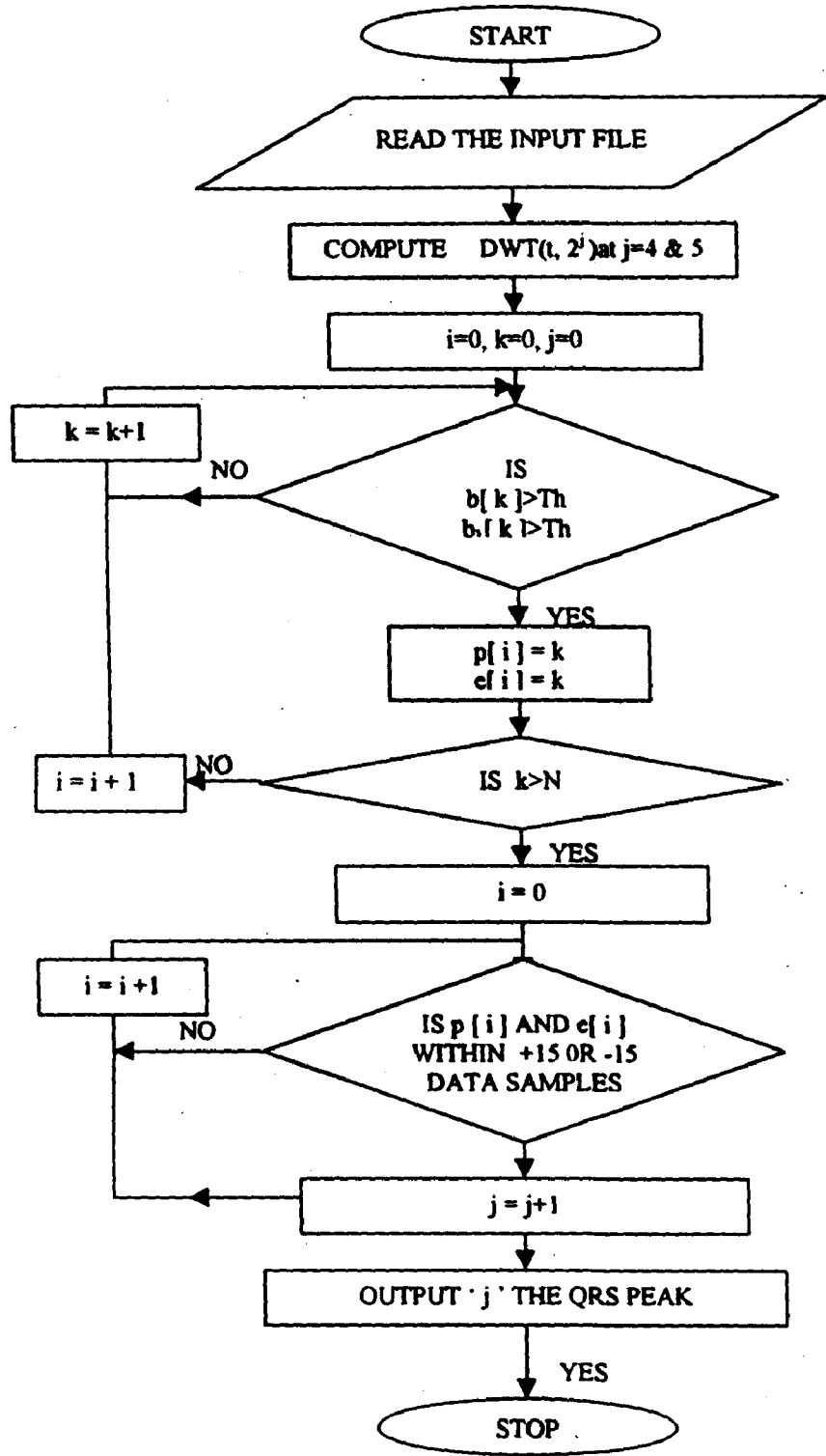
frequency 500 Hz with different frequency components added to it. It is seen that the DWT algorithm worked effectively in separating the different frequency components in corresponding levels of decomposition. The amplitudes of the signals at different levels of decomposition are compared with their known amplitudes and it is seen that they match.

The results of the above algorithm are presented in the next chapter and the flowchart is given in Fig 5.1.

#### **5.4 CONCLUSIONS**

In this chapter, a general discussion on various QRS detection algorithms has been carried out. A DWT based QRS detector is presented in detail stating its advantage over the other QRS detection algorithms.





$b[k]$  → coefficients of detail signal at 4<sup>th</sup> level.  
 $b_1[k]$  → coefficients of detail signal at 5<sup>th</sup> level

Fig 5.1 :Flow Chart for QRS Detection

G10261



---

**RESULTS AND DISCUSSION**

---

**6.1 GENERAL**

The results and a discussion on the algorithms given in chapter 4 and chapter 5 are presented in this chapter. They include

- (i) denoising of ECG signal using Discrete Wavelet Transforms.
- (ii) reduction of baseline wander of ECG using Discrete Wavelet Transforms and
- (iii) Discrete wavelet transform based QRS detector.

The wavelet used for denoising of ECG signal and reduction of baseline wander of ECG signal is Daubechies Wavelet-6 (DB-6) with the coefficients of high pass filter and low pass filter presented in table 3.1 of chapter 3.

As presented in chapter 3, the main process in DWT is the splitting up of the input signal into two parts, one the high frequency are detail signal and the other low frequency or approximation signal. Any wavelet chosen for DWT algorithm splits the input signal as presented in chapter 3. The efficiency of the first two algorithms lies in the selection of the decomposition level for the effective noise removal. Hence one wavelet can be used both for the reduction of high frequency noise and the low frequency noise in the input ECG signal.

All the algorithms are tested using the CSE database.

## 6.2 DENOISING OF ECG SIGNAL USING DISCRETE WAVELET TRANSFORMS

As described in chapter 4, since the noise corresponds to the high frequency component of the ECG signal, the thresholds selected at the three levels considered here are different, with the value at most detailed level relatively high and less with the next two lower levels.

At the detailed level, the threshold is selected as  $\sigma_i \times 2.0$ , where ' $\sigma_i$ ' is the standard deviation at that level,  $i = 1$ .

In the next two lower levels, the thresholds are  $\sigma_i \times 1.5$  and  $\sigma_i \times 0.5$ ,  $i = 2$  and 3, respectively.

The performance of the algorithm is measured based on the root mean square error (RMSE) and percentage root mean square difference (PRD).

Figs 6.1, 6.2 and 6.3 show the signal before and after processing. Figs 6.1 and 6.2 show the input ECG signal corrupted with Gaussian noise and the output signal of the reduction of the noise. The RMSE calculated for the signals in figs 6.1 and 6.2 are 0.04309 and 0.07167 respectively while the PRD calculated are 15.437 and 9.6552 respectively. The RMSE and PRD of the algorithm for the two data files are also shown in the figures. Fig. 6.3 shows the input ECG signal corrupted by noise and the output after noise removal. The RMSE and PRD calculated are 0.0657 and 10.2357 respectively.

Generally if the tolerance range of RMSE is (0 – 0.2), it is acceptable. If the PRD calculated lies in the range (0 – 10) %, it is quite good. If it lies in the range (10 – 15) %, it is also acceptable.

#### 6.4 DISCRETE WAVELET TRANSFORM BASED QRS DETECTOR

The algorithm is tested on two wavelets Daubechies Wavelet-10 (DB-10) and Quadratic Spline Wavelet. The low pass coefficients of (DB-10) are

$$h(0) = 0.160102, h(1) = 0.603829, h(2) = 0.724309, h(3) = 0.138428, \\ h(4) = -0.242295, h(5) = -0.032245, h(6) = 0.07751, h(7) = -0.006241,$$

for a filter of length  $L = 8$

and  $g(L - 1 - n) = (-1)^n \cdot h(n)$ ,  $g(\ ) \rightarrow$  high pass coefficients.

The algorithm is tested on CSE dataset-3 for all 15 lead data of 38 records. The analysis results are given in Table 6.1. Here, 'FP' denotes the number of false positives which corresponds to a detector error of detecting a QRS complex where there is none and 'FN' denotes number of false negatives which corresponds to a detector error of not detecting a QRS complex where there is one.

**Table 6.1**

No. of Beats	Filter length	FP	% FP	FN	%FN
7035	8	13	0.185	222	3.15

For the Quadratic Spline wavelet with the lowpass filter coefficients

$$h(0) = 0.125, h(1) = 0.375, h(2) = 0.375, h(3) = 0.125,$$

and high pass filter coefficients

$$g(1) = -2.0, g(2) = 2.0$$

The analysis results are tabulated in Table 6.2.

**Table 6.2**

No. of Beats	FP	% FP	FN	% FN
7035	-	-	44	0.625

As seen from tables 6.1 and 6.2, the number of FP's incase of DB-10 are 13 and incase of Quadratic spline wavelet are none. Similarly the number of FN's in case of DB-10 and Quadratic spline wavelet are 222 and 44 respectively. By comparing the results of the algorithms given in table 6.1 and table 6.2, it can be stated that the algorithm works effectively for the Quadratic Spline wavelet with the least error of 0.625.

Fig. 6.7 shows the correct QRS peak detection of the input signal with the Quadratic Spline wavelet. Fig. 6.8 shows the accurate detection of QRS peak in the presence of the high amplitude P-wave. Fig. 6.9 shows the false detection of the QRS peaks with (DB-10) wavelet whereas Fig. 6.10 shows the correct detection of the QRS peak with spline wavelet for the same input data file.

Fig. 6.11 shows the accurate detection of the QRS peak in case of the baseline wandering of the input signal.

It shows that the detection of QRS complex is accurate in the presence of the noise such as high amplitude P-wave or baseline drift. It is because the frequency range of these noise signals and that of the QRS complex does not overlap. In case the frequency band of the noise and that of the QRS complex overlap, then it is difficult to detect the QRS complex.

Fig. 6.12 shows the input signal corrupted with both baseline drift and high frequency noise and the output after the reduction of baseline drift. Fig. 6.13 shows the same signal after removal of the high frequency noise

present in it. Fig. 6.14 shows the QRS complex detection of the same signal after the removal of the noise contaminated with it.

## **6.5 CONCLUSIONS**

It can be concluded from the results of the implementation of the algorithms presented in chapter 4 and chapter 5 that the discrete wavelet transform proved to be an effective tool for the reduction of both high frequency and low frequency noise present in the ECG signal and for the accurate QRS complex detection in ECG signal.

---

**CONCLUSIONS AND FUTURE SCOPE OF THE WORK**

---

**7.1 CONCLUSIONS**

In this work, three algorithms based on discrete wavelet transforms have been developed to remove

- (i). The high frequency noise.
- (ii). The low frequency baseline wander and
- (iii). Detect the QRS complex in ECG signal.

All these algorithms were tested on CSE dataset-3. The performance of these algorithms were measured with the help of PRD and RMSE in the case of high frequency noise removal and by the measurement of ECG parameters manually before and after processing incase of baseline wander reduction. It has been seen that the algorithm worked effectively in the removal of high frequency noise with the maximum PRD and RMSE of 16.3145 and 0.22 respectively for 20 records of CSE dataset-3. Regarding the baseline wander reduction, the maximum of 2% change is accounted in measurement of ECG parameters before and after processing. The algorithm also works satisfactorily for the detection of QRS complex in ECG signal with the Quadratic spline wavelet with a least percentage error of 0.625, tested on 38 records of CSE dataset-3.

The advantage of DWT based detection of QRS complex is that it does not assume stationarity within the analysis segment and exhibits robustness to noise. The algorithm presented here is computationally simple.

## 7.2 FUTURE SCOPE

The work can be expanded with respect to the choice of the best wavelet among the available wavelet library or a new wavelet can be suggested. Also the extraction of other features of the ECG signal can be added to the work.



---

## REFERENCES

---

1. Cromwell L., Weibell F. J., Pfeiffer E. A., Biomedical Instrumentation and Measurements, Prentice Hall of India, pp. 10-20, 1999.
2. G. M. Friesen, T. C. Jannett, M. A. Jadallah, S. I. Yatas, S. R. Quint and H. R. Nagle, "A Comparison of the Noise Sensitivity of Nine QRS Detection Algorithms", IEEE Trans. Biomed. Engg., Vol. 37, pp. 85-98, Jan 1990.
3. Devijver, P. A. and Kittler, J., Pattern Recognition : A Statistical Approach, Prentice Hall International, pp. 1-7, 1982.
4. The Wavelet Tutorials by Robi Polikar.  
<http://robipolikar/cl/download/WT.html>
5. Mark P. Wachowiak, Gregory S. Rash, Peter M. Quesada and Ahmed H. Desoky, "Wavelet-Based Noise Removal for Biomechanical Signals : A Comparative Study", IEEE Transactions on Biomedical Engineering, Vol. 47, pp. 360-368, March 2000.
6. Mervin J. Goldman, Principles of Clinical Electrocardiography, LANGE Medical Publication, pp.11-25, 1986.
7. Oliver Rioul and Martin Vetterli, "Wavelets and Signal Processing", IEEE SP Magazine, Vol. 20, pp. 14-34, 1991.
8. Al-Naima and S.C.Saxena, "Computer Aided Technique for the Extraction of ECG Parameters", International Journal of Systems Science, 20, pp. 747-757, 1989.
9. Raghuveer M. Rao, Ajit S. Bopardikar, Wavelet Transforms : Introduction to Theory and Applications, pp. 236-238, 2000.

10. P. A. Lynn, "Online Digital Filters for Biological Signals : Some Fast Designs for a Small Computer", Med. & Biol. Eng. & Comput., Vol.15, pp. 534-540, 1997.
11. P. K. Kulkarni, Vinod Kumar, H. K. Verma, "Removal of Powerline Interference and Baseline Wander Using Real-Time Digital Filter", International Conference on Computer Applications in Electrical Engineering, CERA-97, pp. 2-25, Sept.1997.
12. C. Levkov, G. Michov, R. Ivanov, I. K. Daskaiov, "Subtraction of 50 Hz Interference from the Electrocardiogram", Medical and Biological Engineering and Computing, Vol. 22, pp. 371-373, 1984.
13. M. Okada, "A Digital Filter for the QRS Complex Detection", IEEE Trans. Biomed. Engg., Vol. 26, pp. 700-703, Dec. 1979.
14. Shubha Kadambe, Robin Murray and G. Faye Boudreaux-Bartels, "Wavelet Transform-Based QRS Complex Detector", IEEE Transaction on Biomedical Engineering, Vol. 46, pp. 838-848, 1999.
15. Willis J. Tompkins, Biomedical Digital Signal Processing, Prentice Hall India, pp. 242-245,1999.

RMSE= 0.043092      PRD= 15.437000

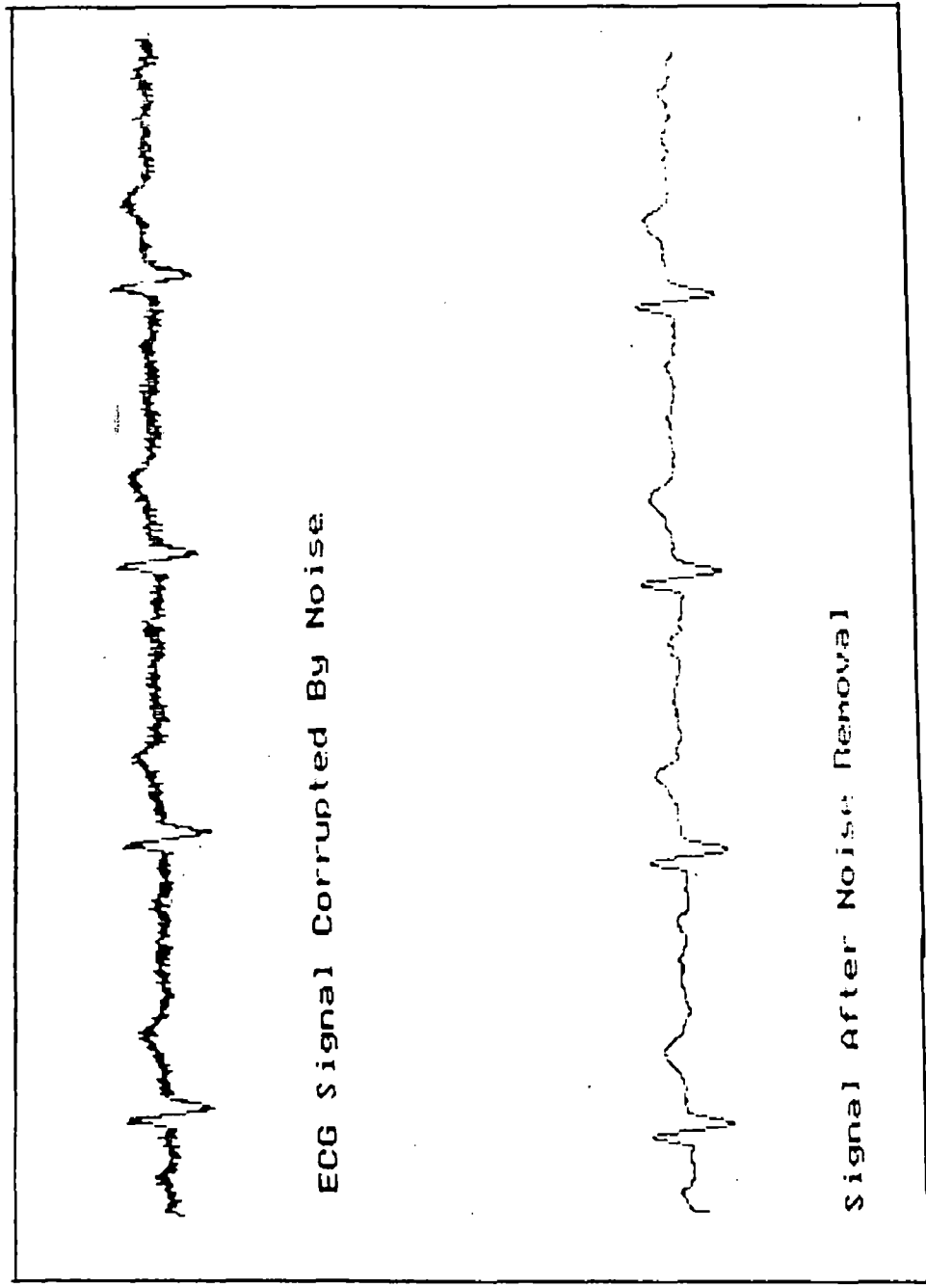


Fig 6.1 Program output for lead L1 data file of first patient for noise removal

RMSE= 0.071676      PRD= 9.655230

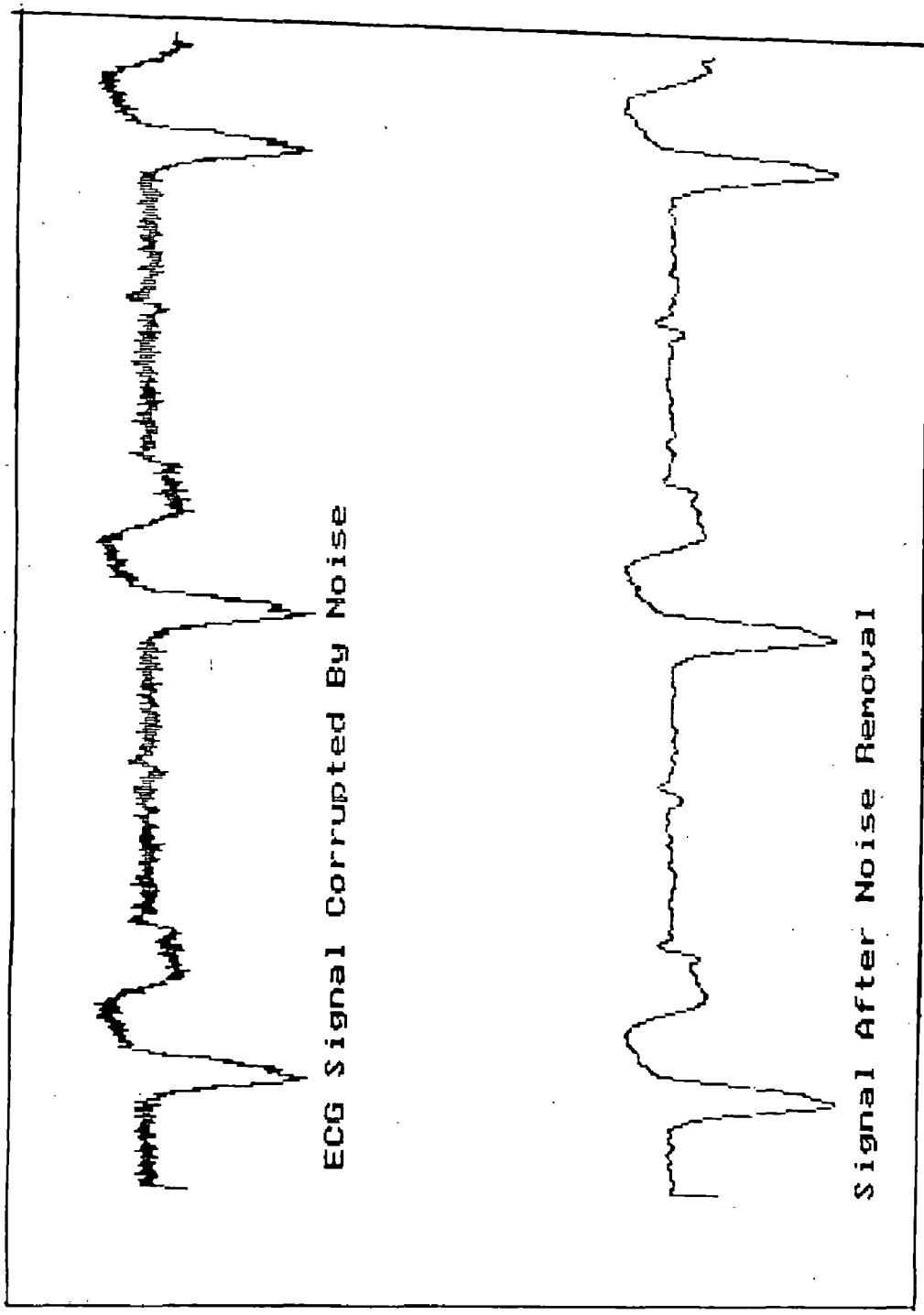


Fig 6.2 Program output for orthogonal lead Z data file of tenth patient for noise removal

RMSE= 0.065739      PRD= 10.235780

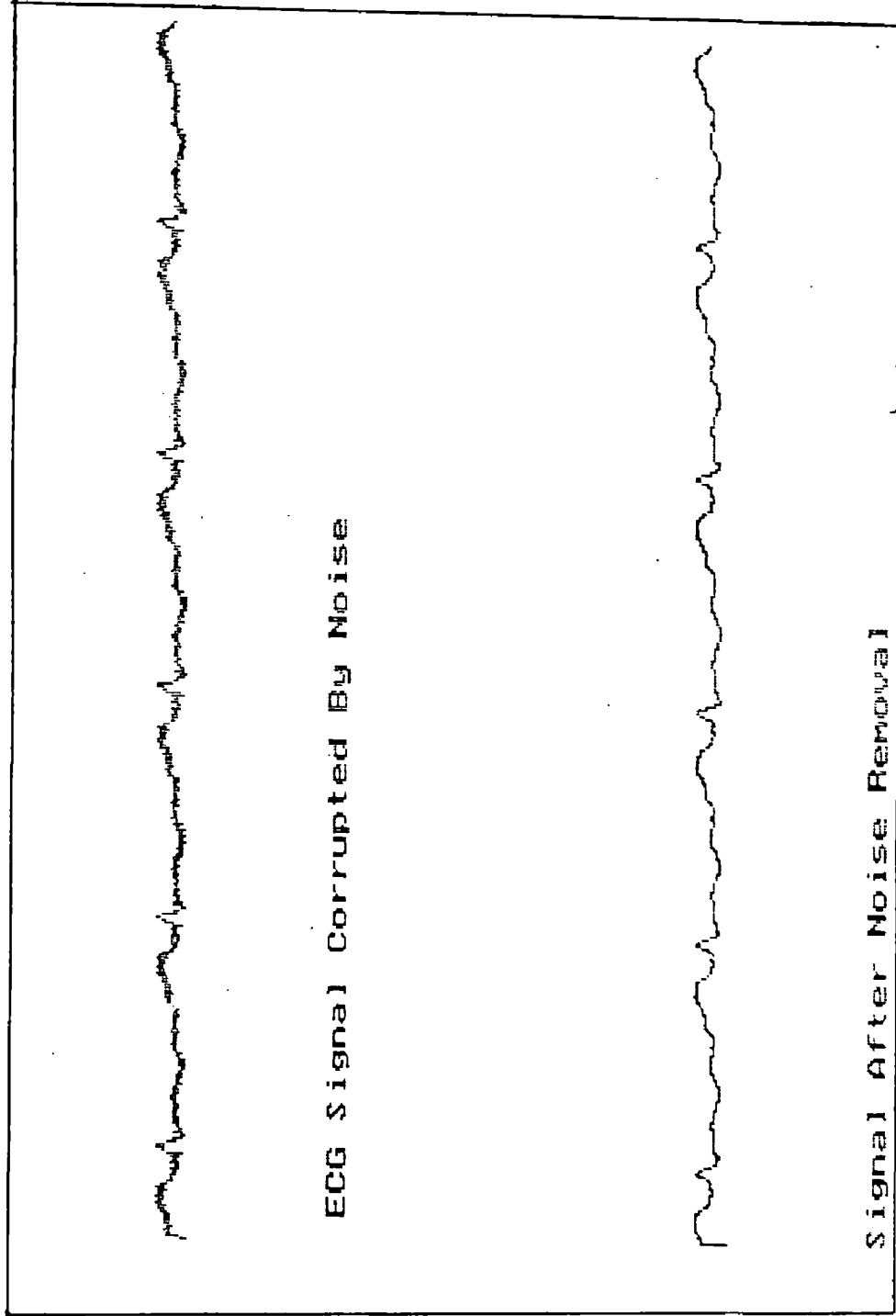


Fig 6.3 Program output for lead L1 data file of twelfth patient for noise removal

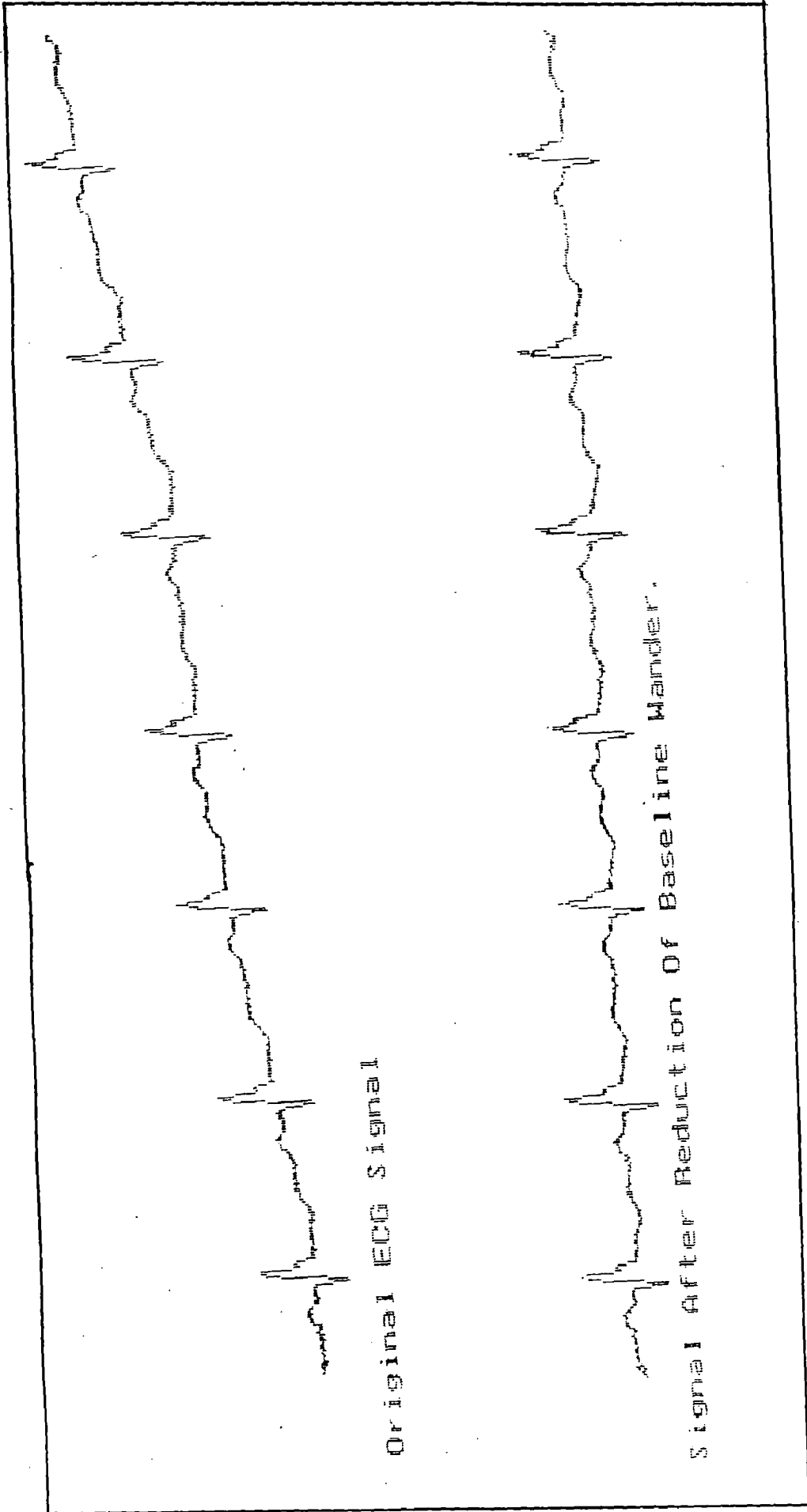


Fig 6.4 Program output for lead V5 diagnostic file of seventh patient for base line wander reduction

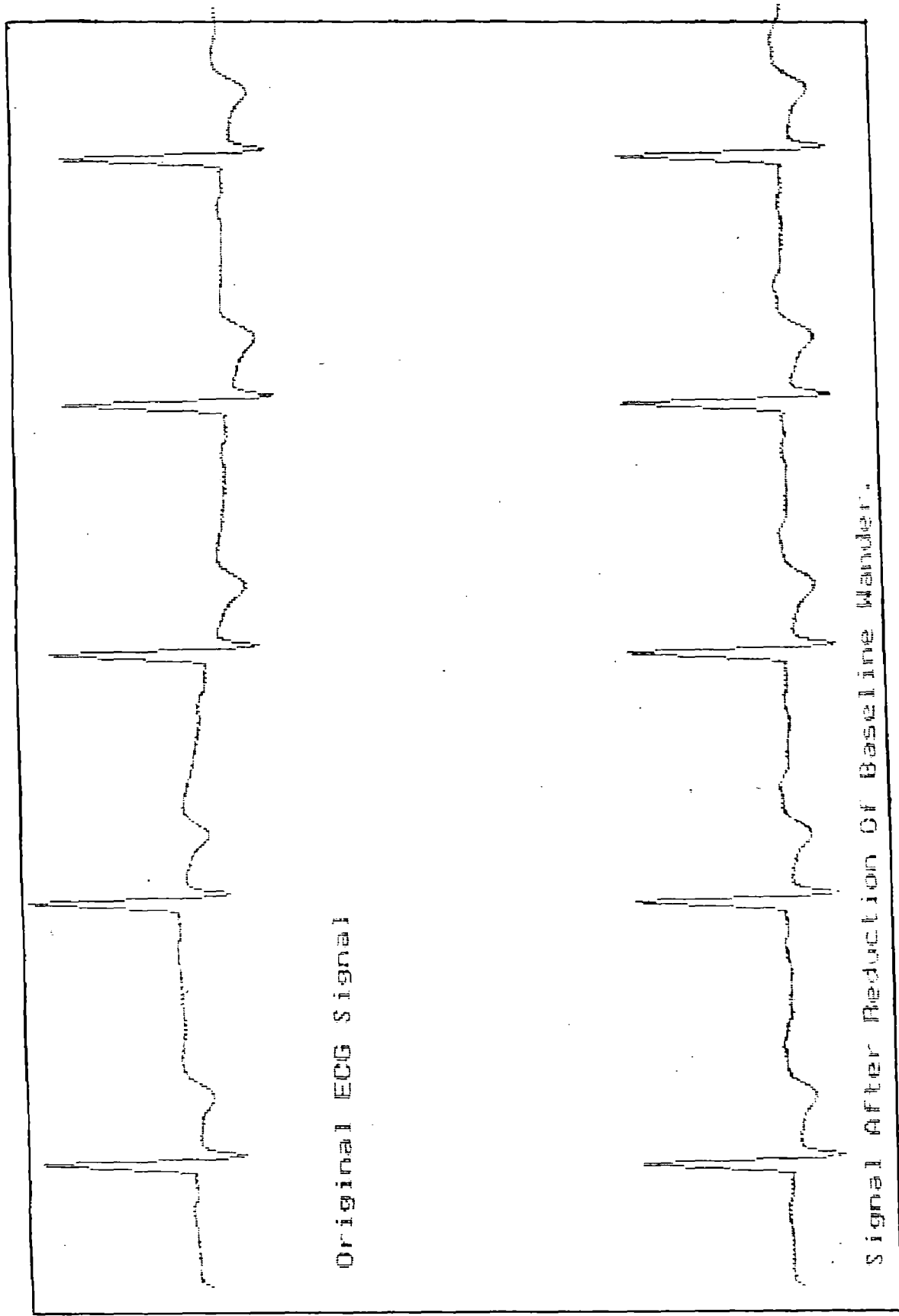
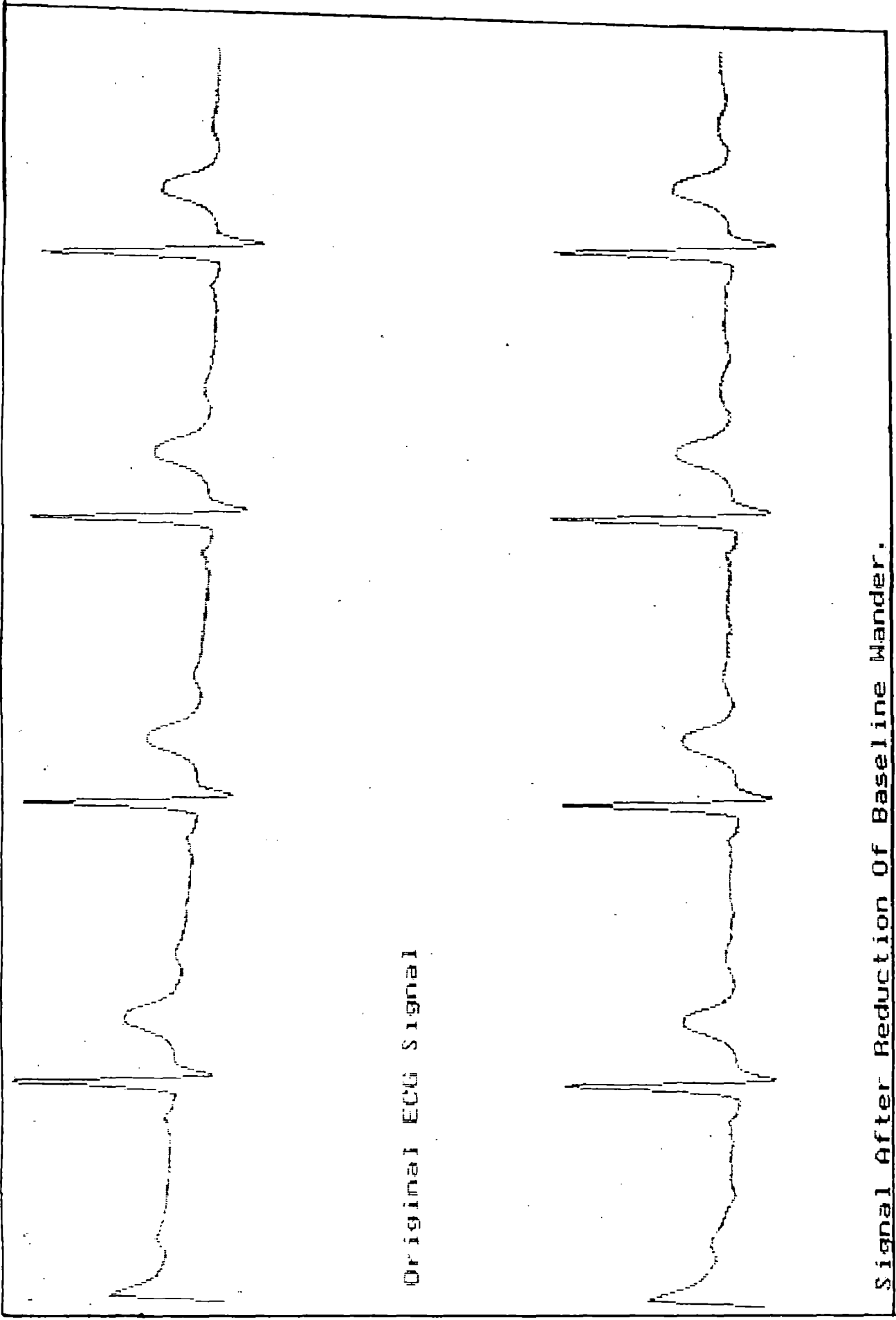


Fig 6.5 Program output for lead V6 data file of eighth patient for base line wander reduction

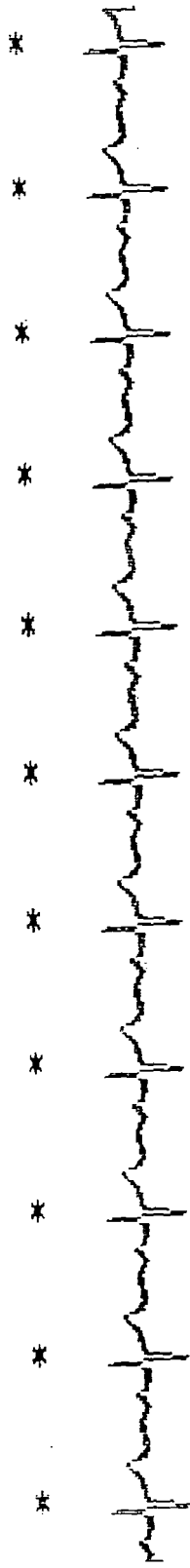


Signal After Reduction Of Baseline Wander.

Fig 6.6 Program output for lead V4 diagnostic file of twelfth patient for base line wander reduction



No of QRS complexes detected = 11



Original ECG signal



Detail signal after fourth decomposition.



Detail signal after fifth decomposition, ' \* ' --> QRS Peak

Fig 6.7 Program output for lead L1 data file of first patient for QRS detection

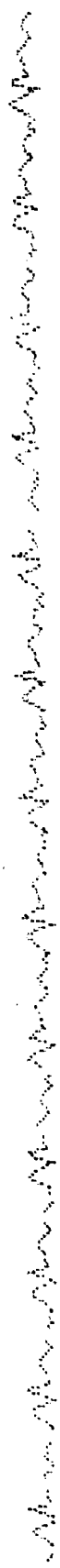
No of QRS complexes detected = 13



Original ECG signal



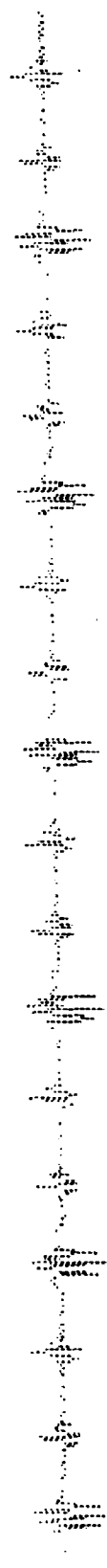
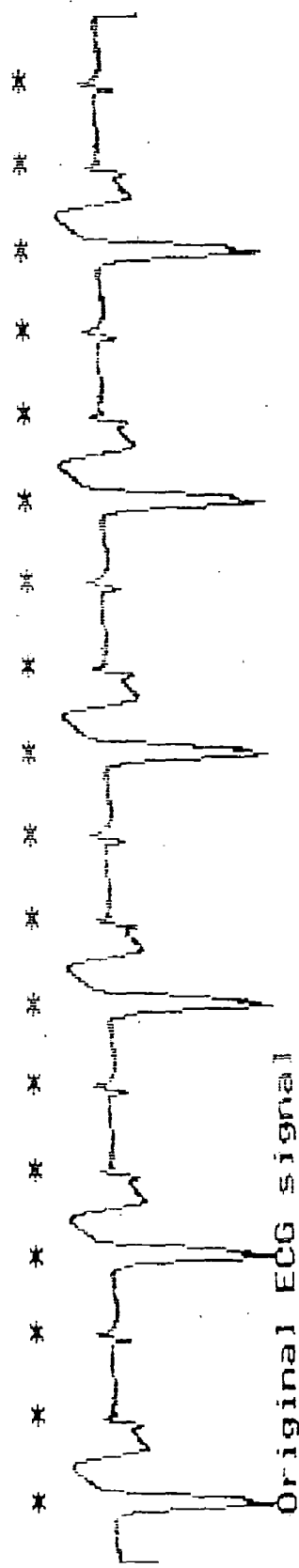
Detail signal after fourth decomposition.



Detail signal after fifth decomposition, \* ' --- > QRS Peak

Fig 6.8 Program output for lead L1 data file of twelfth patient for QRS detection

No of QRS complexes detected = 18



Detail signal after fifth decomposition.



Fig 6.9 Program output for orthogonal lead Z data file of tenth patient for QRS detection

No of QRS complexes detected = 6

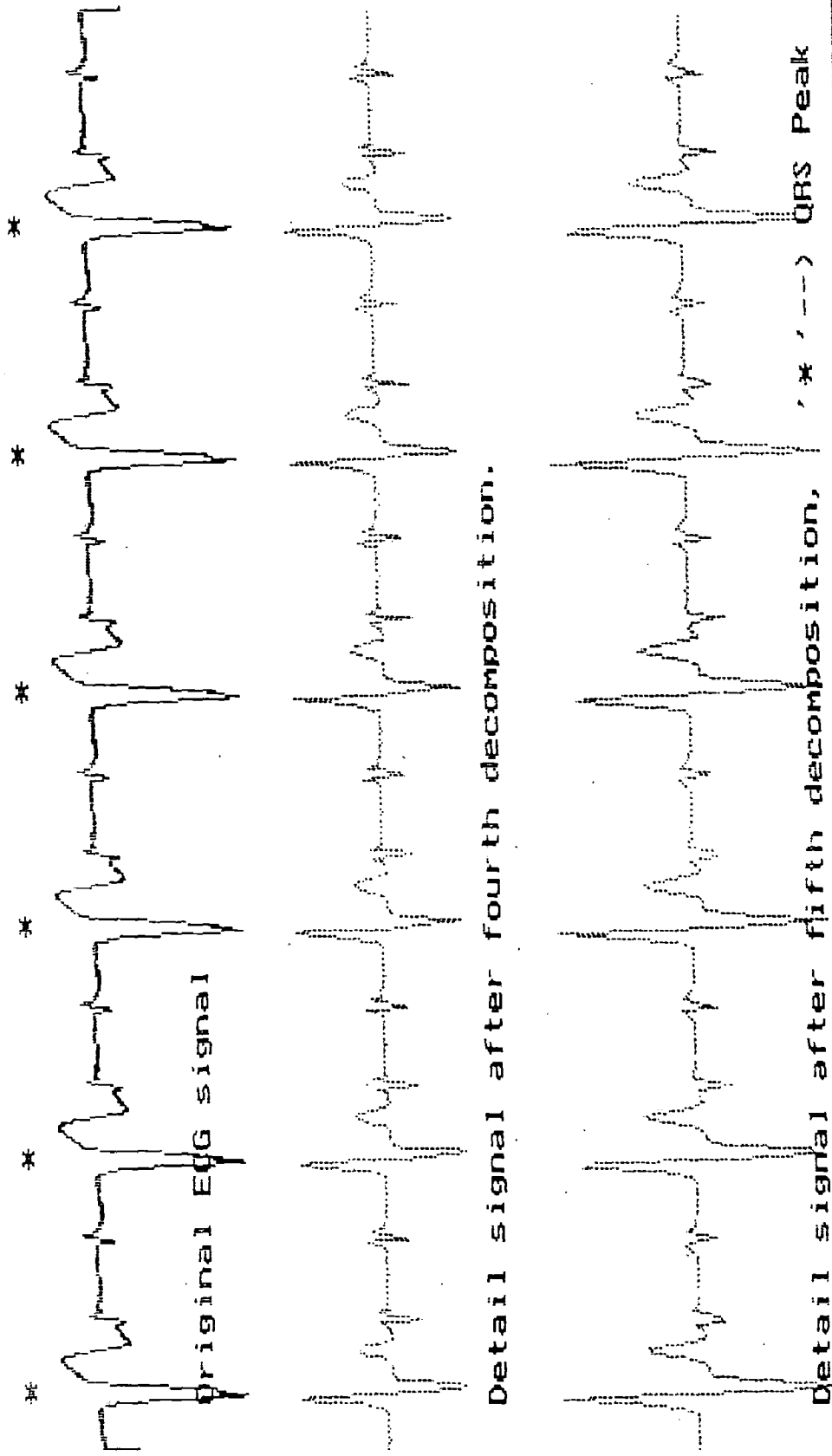


Fig 6.10 Program output for orthogonal lead Z data file of tenth patient for QRS detection

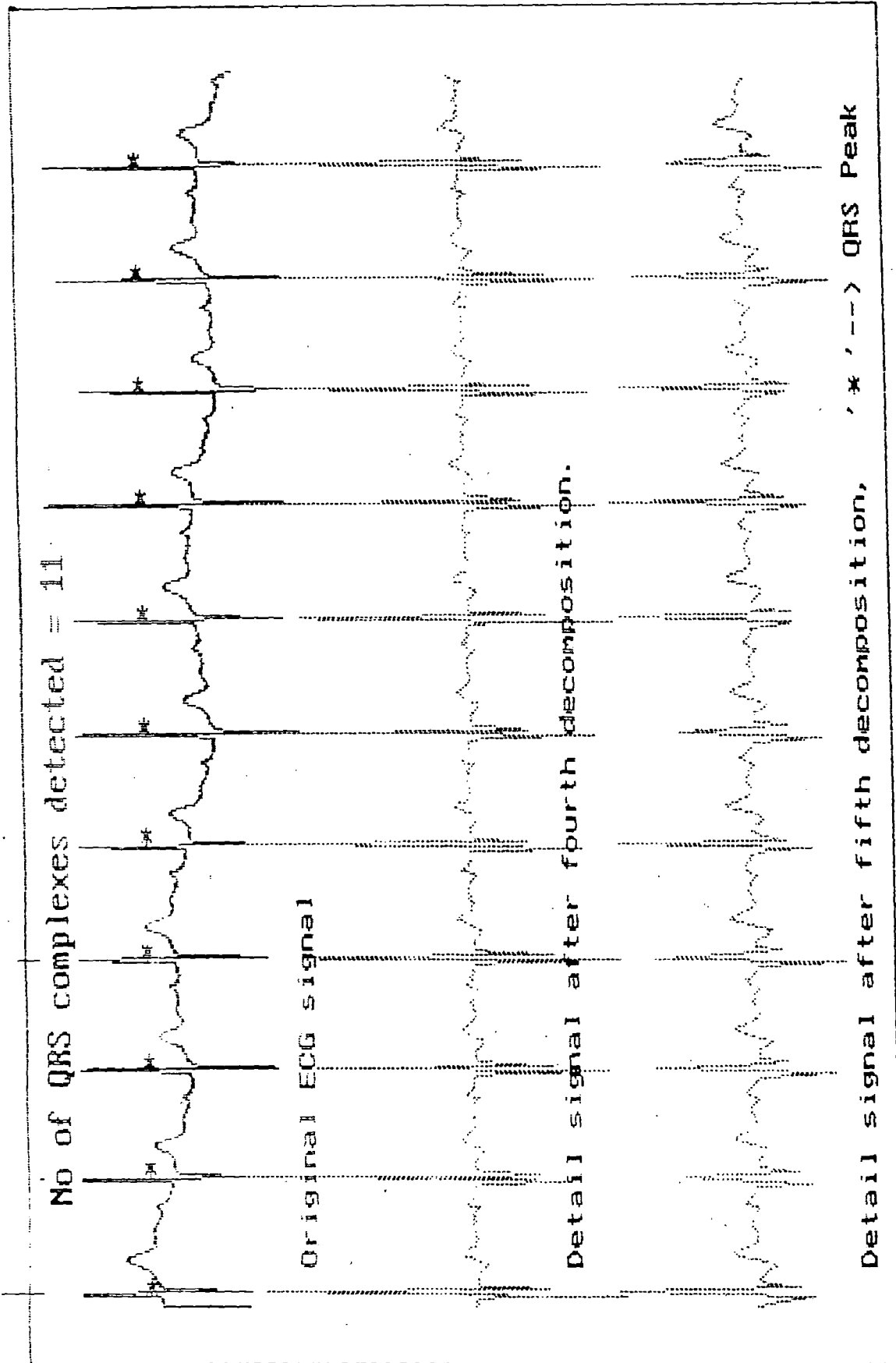


Fig 6.11 Program output for lead V4 diagnostic file of second patient for QRS detection

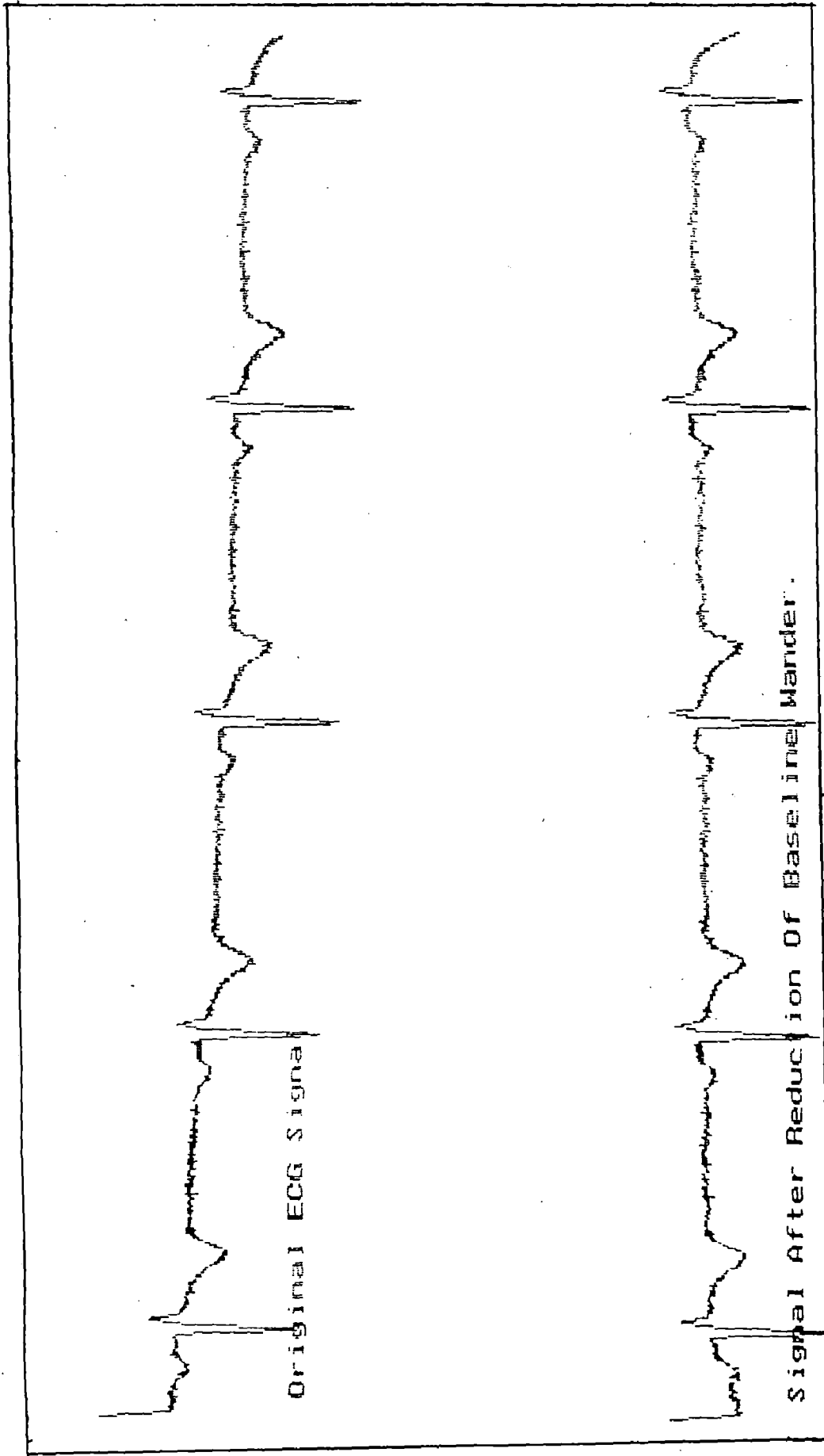


Fig 6.12 Program output for lead aR data file of twenty first patient for base line wander reduction

HRSE-

0.106287

PRD=

13.442595

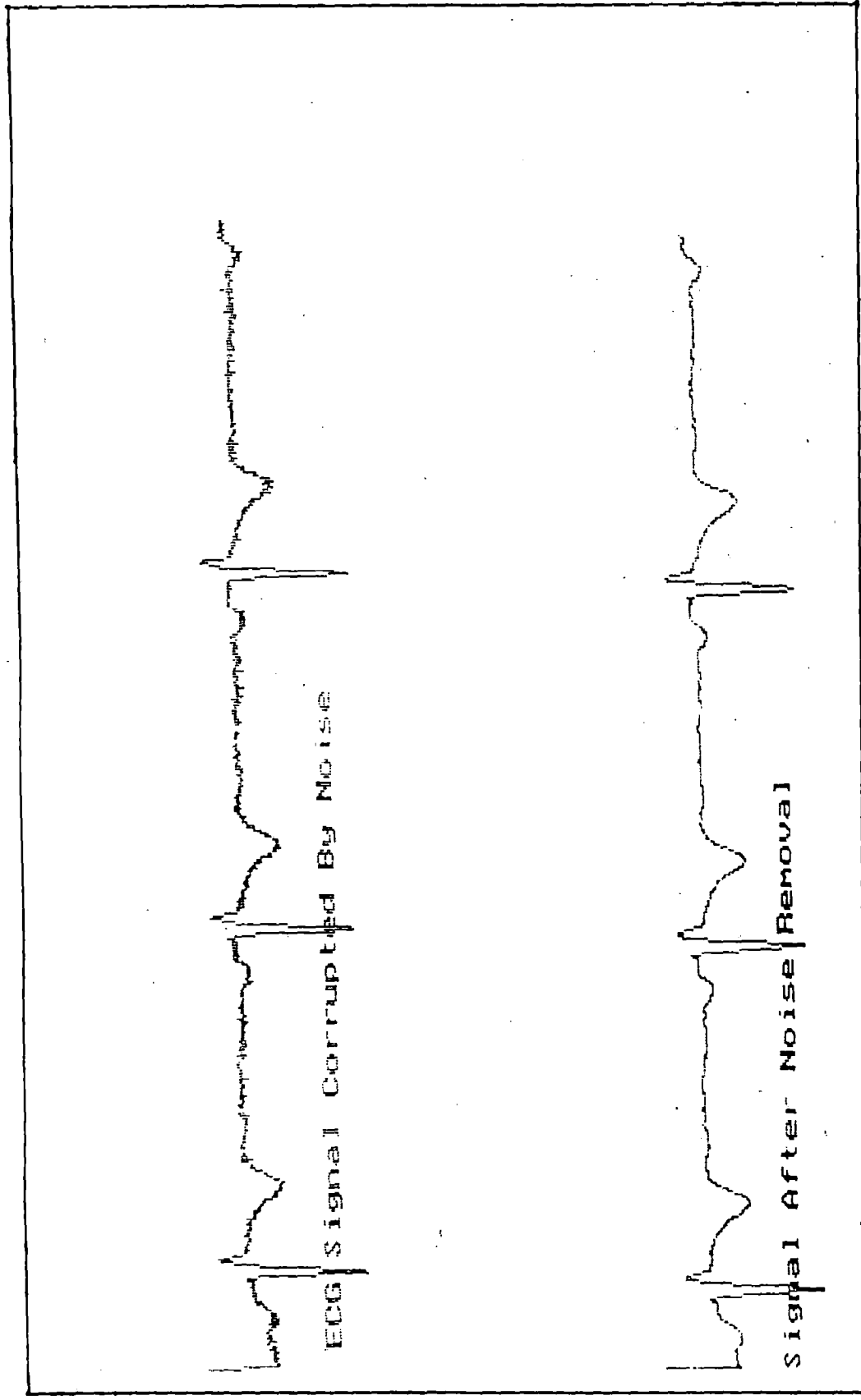


Fig 6.13 Program output for lead aR data file of twenty first patient for noise removal

No of QRS complexes detected = 3

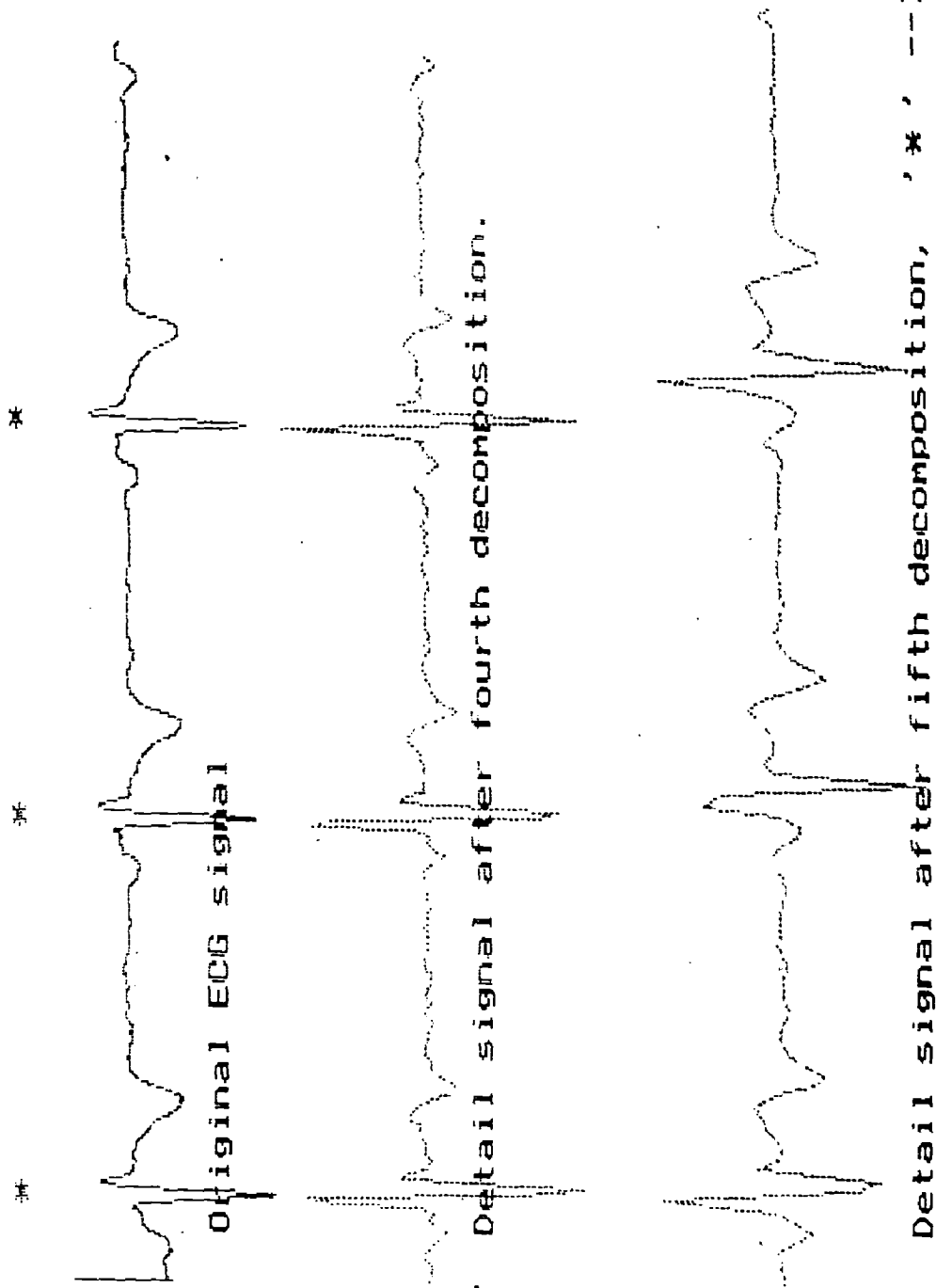


Fig 6.14 Program output for lead aR data file of twenty first patient for QRS detection